Foth C, Evers SW, Pabst B, Mateus O, Flisch A, Patthey M, Rauhut OWM. 2015. New insights into the lifestyle of *Allosaurus* (Dinosauria: Theropoda) based on another specimen with multiple pathologies. PeerJ 3:e940 https://doi.org/10.7717/peerj.940

New insights into the lifestyle of *Allosaurus* (Dinosauria: Theropoda) based on another specimen with multiple pathologies

Christian Foth, Serjoscha Evers, Ben Pabst, Octávio Mateus, Alexander Flisch, Mike Patthey, Oliver W. M. Rauhut

Adult large-bodied theropods are often found with numerous pathologies. A large, almost complete, probably adult Allosaurus specimen from the Howe Stephens Quarry, Morrison Formation (Late Kimmeridgian–Early Tithonian), Wyoming, shows multiple pathologies. Pathologic bones include the left dentary, two cervical vertebrae, one cervical and several dorsal ribs, the left scapula, the left humerus, right ischium, and two left pedal phalanges. These pathologies can be classified as follows: the fifth cervical vertebra, the scapula, several ribs and the ischium are traumatic, and a callus on the shaft of the left pedal phalanx II-2 is traumatic-infectious. Traumatically fractured elements exposed to frequent movement (e.g. the scapula and the ribs) show a tendency to develop pseudarthroses instead of callus healing. The pathologies in the lower jaw and a reduced flexor tubercle of the left pedal phalanx II-2 are most likely traumatic or developmental in origin. The pathologies on the fourth cervical are most likely developmental in origin or idiopathic, that on the left humerus is infectious or idiopathic, whereas left pedal phalanx IV-1 is classified as idiopathic. With exception of the ischium, all traumatic / traumatic-infectious pathologic elements show unambiguous evidences of healing, indicating that the respective pathologies did not cause the death of this individual. Alignment of the scapula and rib pathologies from the left side suggests that all may have been caused by a single traumatic event. The ischial fracture may have been fatal. The occurrence of multiple traumatic pathologies again underlines that large-bodied theropods experienced frequent injuries during life, indicating an active predatory lifestyle, and their survival perhaps supports a gregarious behavior for Allosaurus. Signs of infections are scarce and locally restricted, indicating a successful prevention of the spread of pathogens, as it is the case in extant reptiles (including birds).

PeerJ PrePrints | http://dx.doi.org/10.7287/peerj.preprints.824v1 | CC-BY 4.0 Open Access | rec: 10 Feb 2015, publ: 10 Feb 2015

New insights into the lifestyle of *Allosaurus* (Dinosauria: Theropoda) based on another specimen with multiple pathologies

Christian Foth[1,2] , Serjoscha Evers[2,3], Ben Pabst[4], Octávio Mateus[5,6], Alexander Flisch[7], Mike Patthey[8], Oliver W. M. Rauhut[1,2]

[1] SNBS, Bayerische Staatssammlung für Paläontologie und Geologie, Richard Wagner-Str. 10, D-80333 München

[2] GeoBio-Center, Department of Earth and Environmental Sciences, Ludwig-Maximilians-Universität, Richard-Wagner-Str. 10, D-80333 München, Germany

[3] Department of Earth Sciences, University of Oxford, South Parks Road, Oxford OX1 3AN, UK

[4] Sauriermuseum Aathal, Zürichstr. 69, CH-8607 Aathal-Seegräben, Switzerland

[5] CICEGe, Faculdade de Ciências e Tecnologia, FCT, Universidade Nova de Lisboa, 2829-516 Caparica, Portugal

[6] Museu da Lourinhã, Rua João Luis de Moura, 2530-157 Lourinhã, Portugal

[7] Empa. Swiss Federal Laboratories for Materials Science and Technology, Center for X-ray Analytics, Überlandstrasse 129, CH-8600 Dübendorf, Switzerland

[8] Vetsuisse Fakulty, Universität Zürich, Winterthurerstrasse 260, CH-8057 Zürich, Switzerland

PeerJ PrePrints | http://dx.doi.org/10.7287/peerj.preprints.824v1 | CC-BY 4.0 Open Access | rec: 10 Feb 2015, publ: 10 Feb 2015

Abstract

Adult large-bodied theropods are often found with numerous pathologies. A large, almost complete, probably adult *Allosaurus* specimen from the Howe Stephens Quarry, Morrison Formation (Late Kimmeridgian–Early Tithonian), Wyoming, shows multiple pathologies. Pathologic bones include the left dentary, two cervical vertebrae, one cervical and several dorsal ribs, the left scapula, the left humerus, right ischium, and two left pedal phalanges. These pathologies can be classified as follows: the fifth cervical vertebra, the scapula, several ribs and the ischium are traumatic, and a callus on the shaft of the left pedal phalanx II-2 is traumatic-infectious. Traumatically fractured elements exposed to frequent movement (e.g. the scapula and the ribs) show a tendency to develop pseudarthroses instead of callus healing. The pathologies in the lower jaw and a reduced flexor tubercle of the left pedal phalanx II-2 are most likely traumatic or developmental in origin. The pathologies on the fourth cervical are most likely developmental in origin or idiopathic, that on the left humerus is infectious or idiopathic, whereas left pedal phalanx IV-1 is classified as idiopathic. With exception of the ischium, all traumatic / traumatic-infectious pathologic elements show unambiguous evidences of healing, indicating that the respective pathologies did not cause the death of this individual. Alignment of the scapula and rib pathologies from the left side suggests that all may have been caused by a single traumatic event. The ischial fracture may have been fatal. The occurrence of multiple traumatic pathologies again underlines that large-bodied theropods experienced frequent injuries during life, indicating an active predatory lifestyle, and their survival perhaps supports a gregarious behavior for *Allosaurus*. Signs of infections are scarce and locally restricted, indicating a successful prevention of the spread of pathogens, as it is the case in extant reptiles (including birds).

Subjects Animal Behavior, Paleontology, Pathology, Veterinary medicine, Zoology

Keywords Archosauria, gregarious behavior, Jurassic, osteomyelitis, paleopathology, pseudarthrosis, Theropoda

Introduction

Palaeopathology is the study of diseases and traumatic injuries in extinct animals and reveals great potential to provide insights into behaviour (e.g. Rothschild & Storrs, 2003), physiology (e.g. Rothschild et al., 2003), life history (e.g. Hanna, 2002) as well as interspecific (e.g. predator-prey relationships) and intraspecific interactions (e.g. intraspecific combats) (e.g. Carpenter, 2000; Tanke & Currie, 2000; Avilla, Fernandes & Ramos, 2004; Farke, 2004; Carpenter et al., 2005; Farke & O'Connor, 2007; Butler et al., 2013). In recent years, the study of osteological pathologies among non-avian dinosaurs has become of great interest, documenting a wide range of different kinds of injuries and diseases, e.g. fractures and stress fractures (Rothschild, 1988; Rothschild, Tanke & Ford, 2001; Hanna, 2002; Anné et al., 2014), amputations (Farke & O'Connor, 2007; Butler et al., 2013), bite marks and scratches (Carpenter, 2000; Tanke & Currie, 2000; Peterson et al., 2009; Bell, 2010), cancer and tumour growth (Rothschild et al., 2003; Arbour & Currie, 2011), developmental disorders (Witzmann et al., 2008) as well as different kinds of microbial infections (Hanna, 2002; Wolff et al., 2009; Witzmann et al., 2011). Of special interest in this respect are non-lethal pathologies, as they can potentially tell us something about the lifestyle of the animal. Especially, large-bodied non-avian theropods are frequently found with numerous fractures, bite marks and infections (Gilmore, 1920; Molnar & Farlow, 1990; Molnar, 2001; Hanna, 2002; Brochu, 2003; Farke & O'Connor, 2007; Rothschild & Molnar, 2008; Bell, 2010; Bell & Coria, 2013), indicating an active predatory life style predisposed to injuries (Hanna, 2002). The basal tetanuran *Allosaurus* is one of the best-documented dinosaurs in this field of research (e.g. Marsh, 1884; Gilmore, 1920; Moodie, 1923; Petersen, Isakson & Madsen, 1972; Madsen, 1976; Rothschild, 1988; Rothschild & Martin, 1993; Hanna, 2002; Anné et al., 2014). However, only one study, which is based on the almost complete *Allosaurus* specimen MOR 693 ('Big Al') as well as isolated material from the Cleveland-Lloyd Dinosaur Quarry, has studied its pathologies in greater detail and in a comparative approach (Hanna, 2002). Here, we report a second almost complete, probably adult *Allosaurus* specimen from the Upper Jurassic of Wyoming, U.S.A, which possesses several pathologic bones, including the left dentary, two mid-cervical vertebrae, a right cervical rib, several dorsal ribs, the left scapula, the left humerus, the right ischium, and the left pedal phalanges II-2 and IV-1 (Fig. 1). After documentation and diagnosis, the single pathologies of the specimen will be compared with the data from Hanna (2002) and that of other large-bodied theropods, so that the current study provides new insights into the disease patterns and lifestyles of these remarkable predators.

Material and Methods

The *Allosaurus* specimen SMA 0005 ('Big Al 2') was collected from the Upper Jurassic outcrops of the Morrison Formation (Late Kimmeridgian – Early Tithonian) of the Howe Ranch (Howe Stephens Quarry), Big Horn County, Wyoming, by a team of the Sauriermuseum Aathal (Switzerland) in 1996, close to the famous Howe Quarry discovered by Barnum Brown in 1934 (Brown, 1935; Breithaupt, 1997). The almost complete skeleton was found partially articulated and probably represents an adult individual (total body length = 7.6 m), which is about 12% larger than MOR 693 ('Big Al'), which was found only a few hundred meters away.

For classification of different pathologies present in SMA 0005 we follow the nomenclature of Hanna (2002), who classifies osteological abnormalities as 1) traumatic (resulting from traumatic injury), 2) infectious (resulting from viral, bacterial and protozoan infection), 3) traumatic-infectious (resulting from secondary infection of an injured element), 4) developmental (caused by growth disturbance during development), and 5) idiopathic (pertaining to a condition without clear pathogenesis).

Traumatic injuries of bone include fractures and amputations. If these injuries do not cause the immediate death of an animal they are characterized by healing responses, usually in form of callus formation (Cleas, Wolf & Augat, 2000), which is proliferating growth of originally non-mineralized connective tissue to close the gap and stabilize the respective injury (Park et al., 1998; Cleas et al., 2000; Schell et al., 2005). Generally, the callus surrounds the perimeter of the injured bone locally and forms a different superficial structure compared to healthy bone. If the healing process of the injury is not disturbed by secondary infections or interfragmentary movements, the callus is remodelled by zonal lamellar bone after some time (McKibbin, 1978; Park et al., 1998). In case of bone fractures, however, intense mechanical loadings and interfragmentary movements can rupture the bridging callus tissue, including its vessels, resulting in the formation of a pseudarthrosis or ‘false joint’ (Cleas et al., 2000; Loboa, Beaupré & Carter, 2001; Klein et al., 2003; Strube et al., 2008), which is usually accompanied by chronic pain, and often so by disability (Loboa et al., 2001). However, pseudarthrosis can also result from syntraumatic malunions (Klein et al., 2003).

An osteological abnormality caused by viral, bacterial or protozoan infections is called osteitis. If such infection becomes chronic and affects the bone marrow it is called osteomyelitis (Pschyrembel, 1990), which is usually characterized by comb-like lesions on the bone surface. In extant mammals, tissue-invasive microbial infections are often characterized by locally restricted, subperiostal suppurative abscesses. In later stages, these abscesses can cause necroses of original bone due to an infiltration of pus into the blood vessel system, impairing the blood supply of the local bone area. Such infiltrations can further lead to a spread of microbial pathogens via the blood stream, affecting other skeletal elements (so called haematogenous osteomyelitis) (Ortner & Putschar, 1981; Pschyrembel, 1990; Gross, Rich & Vickers-Rich, 1993). In contrast, extant reptiles (including birds) do not respond to tissue-invasive microbial infections by producing liquid pus (Montali, 1988; Rega, 2012), but instead by exuding fibrin into the infected areas, which forms local fibriscesses (as a type of granuloma), and preventing the spread of the infection via the blood stream (Gomis et al., 1997; Huchzermeyer & Cooper, 2000; Cooper, 2005). Thus, reptiles usually manifest only contiguous osteomyelitis. Besides osteomyelitis, osteitis can also lead to the formation of exostoses, superficial bony outgrowths.

Developmental disorders are pathologies related to ontogenetic abnormalities resulting from inherent genetic defects or growth disturbances, whereas in idiopathic abnormalities the cause of the osteological pathology is unknown (Hanna, 2002).

To study potential internal structures several pathologic bones of SMA 0005 were CT scanned. The left dentary and the left scapula were investigated using a Siemens SOMATOM Sensation Open (CT) system at Vetsuisse Faculty (University of Zurich) with source: 120 kV, 176 mA, rotation time: 1 s, pitch: 0.55 mm and slice thickness: 0.6 mm. The fifth cervical was scanned with a 450kV X-ray system MG450 (YXLON) and a CITA 101B+ collimated line detector (CITA Systems Inc.) at the Center for X-ray Analytics (EMPA, Swiss Federal Laboratories for Materials Science and Technology) with source: 450 kV, 3.3 mA, focal spot size: 2.5 mm, target: wolfram, 750 projections of 0.04 s over 360°, slice thickness: 0.25 mm. The generated CT data were preceded with help of the 3D reconstruction software package Amira 5.3.3 (Visage Imaging, Inc.). Unfortunately, the foot was firmly installed in the mounted skeleton, so that the pathologic phalanges could not be scanned.

Institutional Abbreviations

BSPG, Bayerische Staatssammlung für Paläontologie und Geologie, München, Germany; **BYU**, Earth Science Museum, Brigham Young University, Provo, U.S.A.; **DINO** Dinosaur National Monument, Vernal, U.S.A.; **MOR**, Museum of the Rockies, Bozeman, U.S.A.; **NCSM**, North Carolina Museum of Natural Sciences, Raleigh, U.S.A.; **SMA**, Sauriermuseum Aathal, Switzerland; **UMNH**, Utah Museum of Natural History, Salt Lake City, U.S.A., (formerly UUVP, University of Utah Vertebrate Paleontology); **USNM**, National Museum of Natural History, (formerly United States National Museum), Smithsonian Institution, Washington, D.C., U.S.A.

Results

Dentary

The anterior end of the left dentary in SMA 0005 is strongly modified. In lateral view, it has the shape of an anterior rosette, similar to the morphology seen in spinosaurid megalosaurs (Stromer, 1915; Charig & Milner, 1997; Sereno et al., 1998). The anterior part is both dorsally and ventrally expanded, reaching a maximal height at the level of the fifth alveolus. Anteriorly, the alveolar border curves ventrally, forming a convex arch, resulting in a slightly procumbent anterior-most and, to a lesser degree, second alveolus (Fig. 2). Anterior to the first clearly identifiable alveolus, there is another concavity on the medial side of the bone facing anterodorsally, which might represent a further tooth position. If this interpretation were correct, the first tooth of the left dentary in SMA 0005 would be almost anteriorly directed. However, CT data of the dentaries show that the proximal part of the left dentary is formed by compact bone, while respective parts on the right dentary, as well as more distal parts on both dentaries, show repetitive indentations representing deep alveoli. Therefore, it is also possible that the first alveoli of the left dentary were reduced during the healing response to merely externally visible, shallow pits, and that the anterior part of the left dentary was thereafter edentulous. No clear indication of a fracture, bite marks, callus or other lesion are visible, indicating that this pathology happened a long time before the death of the animal, possibly even during its early development. As a consequence of the pathology in the left dentary, the symphysial region of the mandible is dorsoventrally shortened, and when both mandibles are aligned with the ventral border of the symphysis, at least the anterior part of the left alveolar margin would project dorsally well beyond the right alveolar margin.

Cervicals

Within the cervical series of SMA 0005 two cervical vertebrae could be identified as pathologic. The fourth cervical shows a conspicuous, irregularly shaped proliferation of bone originating from the posteromedial side of the left prezygapophysis (Fig. 3A, B). The proliferation is anteroventrally and medially directed and measures c. 9 mm anteroposteriorly, c 18 mm dorsoventrally and 25 mm lateromedially in its maximum extent. Anteriorly, the proliferation flattens and expands laterally, contacting the ventromedial side of the left prezygapophysis, so that it looks inverted L-shaped from dorsal view. From anterior view it is kidney-shaped with the concave edge facing ventrally. The surface of the structure is overall rugose. A further small anomaly is present medial to the left lateral margin of the spinopostzygapophyseal fossa above the neural canal (Fig. 3C-E). The structure is posteroventrally directed and tapers distally. It measures c. 6 mm anteroposteriorly, c. 9 mm dorsoventrally and c. 11 mm lateromedially. A clear diagnosis of both exostoses is difficult. As no external indicator of a fracture or infection is observable, and as the structures belong to none of the regular parts and processes of the vertebra, the most plausible explanation could be an enthesopathy (= inflammatory ossification of ligamentous or muscular attachments), an osteochondroma (= benign bone tumour) or an idiopathy. Here, the irregular shape of the large anterior exostosis may correspond with the cauliflower-like morphology of an osteochondroma (Murphey et al., 2000).

The neural arch of the fifth cervical shows a severe injury caused by a fracture at the base of the left postzygapophysis (Fig. 4). In external view, the fracture runs around the whole process, indicating the complete rupture of the postzygapophysis. The fracture is surrounded by a large callus on the dorsolateral side, which gives the left postzygapophyseal pedicle a swollen appearance, and follows roughly the course of the epipoprezygapophyseal lamina. While the broken postzygapophyseal fragment seems secondarily well connected to the neural arch medially, the fracture line appears as a gap laterally, separating the callus in an anterior and posterior part, which are not connected to each other. The anterior part of the callus measures c. 38 mm. Anteriorly, it ends at the level of the posterior edge of the transverse process. The callus shows a stronger lateral (c. 14 mm) than dorsal expansion (c. 8 mm). The posterior part of the callus is smaller and measures c. 19 mm in its anteroposterior dimension. The external surface of both parts of the callus is smooth, without any rugosity. CT data of the specimen show no abnormalities in the bone structure around the injury.

Presacral ribs

Several ribs of SMA 0005 show evidence of traumatic events. In the cervical region, one pathologic rib is found on the right side of the fourth cervical vertebrae (Fig. 5A). In the dorsal region, the fifth rib from the right body side shows a fracture in its distal third. On the left body side, the third, seventh and ninth dorsal ribs show clear evidences of fractures, appearing all in the distal half of the rib, almost on the same level (Fig. 5B). Other ribs from the left side also show deformations on this level. However, as clear fractures cannot be observed, a distinction between a pathologic or taphonomic origin is not possible for the deformed elements. All fractured bones identified show a distinct overlapping connection of both broken elements, sometimes with a slight displacement of the distal end. No callus formation is visible. These observations are consistent with the morphology of pseudarthroses (Cleas et al., 2000; Loboa et al., 2001; Klein et al., 2003).

Scapula

A complete, transverse fracture occurs in the proximal part of the left scapula (Fig. 6). This fracture does not show a regular callus, but some osseous connection of the fractured end to the respective other fragment is apparent. Thus, the proximal fragment, which articulates with the coracoid and the humerus, is laterally displaced, so that it sits on the distal fragment. The periphery around the distal end of the proximal fragment shows a rough striation in line with the longitudinal axis of the scapula. The lateral displacement may be explained by a number of reasons, including mechanical instability due to the morphology of the scapula as a blade-like element or the nature of the traumatic event that caused the fracture. One possible explanation might be found in the separation of muscle groups on the lateral scapula in a distal part (*M. deltoideus scapularis*) and a more proximal part (*Mm. scapulohumeralis, M. deltoideus clavicularis*), with the boundary between these two regions apparently coinciding with the area of the break in SMA 0005 (see Remes, 2008; Burch, 2014). Thus, the pull of the *M. deltoideus scapularis* would have rotated the distal end of the scapula outwards in respect to the proximal end, possibly accounting for the overlap. Furthermore, the proximal fragment is displaced in that it is rotated ventrally. This tilt is probably caused by the mechanical load of the arm, pulling the fragment it is articulated with down. The malunion of the fracture fragment, once achieved, can hardly be reversed, and the weight of the attached arm together with movements induced by arm use and torso movements related to locomotion of the animal account for a lack of stabilization of the fracture. The maximal overlap between the proximal and distal element is c. 81 mm. CT data of the specimen show that most of the overlapping parts only lie on top of each other, and that only the fracture ends constitute a fused bridge between the fracture elements (Fig. 6D). The overall morphology and the CT data of the fracture are consistent with the morphology of a pseudarthrosis (Cleas et al., 2000; Loboa et al., 2001; Klein et al., 2003). In a preliminary report (Evers et al., 2013), we described a second potential fracture of the scapula in the distal part of the bone. However, a re-examination of the specimen suggests rather a plastic deformation of this structure.

Humerus

The left humerus of SMA 0005 shows an abnormal ulnar condyle (Fig. 7). The ulnar condyle has an irregular surface texture of numerous pits of varying depth, and it has a deep oblique groove toward the anterior aspect of the medial side. Additionally, the ventral surface of the ulnar condyle bears some sharp, trough-like marks. Also, the ulnar condyle of the left element is elongate and thin, contrasting the more rounded morphology usually seen in theropods and also seen in the right element. Therefore, the abnormal form and texture of the left ulnar condyle is interpreted as an idiopathic pathology, although the pits might indicate a potential infection.

Ischium

The right ischium exhibits an oblique fracture located at a midshaft position (Fig. 8). The distal fracture fragment sits on the medial side of the proximal fragment, and is slightly medially rotated. Due to this orientation, there is a distally widening interfragmentary gap between the distal end of the proximal fracture fragment and the proximal part of the distal fracture fragment, which can be best seen in anterior view (Fig, 8B). Consequentially, the end of the proximal fragment forms a laterally projecting tip. The gap is partially filled with matrix, which shows that is was internally not closed by connective tissue when the animal died. The fracture line can be traced almost around the entire shaft of the ischium (Fig. 8B-E). However, toward the proximal end of the fracture, the fragments are well connected on the anteromedial side. Because no clear callus structure is visible, and because the fracture line is at no point bridged by cortical bone, it is possible, that either the trauma caused only incomplete fracturing and no healing took place (which would indicate trauma-related death of the animal), or that breakage of the bone occurred post-mortem. Another possibility is that the fracture was complete, and that the anteromedially located connection of the fragments was secondarily achieved. In this case, the structure would fulfill the criteria of a developing pseudarthrosis (see Cleas et al., 2000; Loboa et al., 2001; Klein et al., 2003). On the anterior side of the fractured area, the cortical surface is disturbed by a large trace of small, interconnected depressions with irregular size, shape, and depth. The traces continue well beyond the fracture almost to the ischial boot. As similar traces appear also on the surface of other bones we interpret this structure as most probably taphonomic in origin (see discussion, Fig. 5C, D).

The left ischium shows a slight swelling and possible associated fracture line at the same level as the right element (Fig. 8A). However, parts of the possible pathology are obscured by a reconstruction of the lateral bone surface in this part. Thus, if our observation is correct, it would be impossible to say if the bone was completely or only partially fractured, and if any healing occurred. However, due to the present uncertainty regarding this structure, we avoid further interpretations.

Foot

The pedal phalanx II-2 of the left foot has a bulbous callus covering about two-thirds of the element (Fig. 9A-D). The callus is located at the proximal part of the phalangeal shaft, and does not reach both the proximal and distal articulation facets. In the mid-shaft area, the callus surrounds the phalanx body almost entirely. Toward the proximal articulation, the callus forms a groove-like channel with a sharp and step-like edge, which circumferences the medial, dorsal, and lateral parts of the callus. Towards the distal articulation, the callus is laterally complanate and hence approaching the regular morphology again, while the medial aspect is strongly swollen. The ventral side of the proximal end is also strongly inflated, exhibiting a c. 5 mm thick bulge. The surface of the callus is generally irregular, while the degree of irregularity is reducing towards the distal part of the element, and weaker developed than in comparative specimens (Hanna, 2002; see discussion).

Compared to the non-pathological pedal phalanx II-2 of the right foot (Fig, 9E), the extensor tubercle is almost completely reduced in the left pedal phalanx II-2 with the most proximal point ending approximately 40 mm anteriorly in relation to the ventral flexor heel (see Fig, 9A, C, D). However, the surface structure in the respective area of the phalanx is not indicative of taphonomic deformation or erosion. Therefore, this anomaly likely represents a pathologic structure. It is perhaps developmental in origin or results from a healed trauma that happened a long time before the death of the animal.

Several depressions could be observed in this bone, penetrating the callus (Fig. 9B, C). The largest depressions appear posteromedially and are several millimetres deep. Here, the outer margin of the more posterior depression measures c. 6 mm by 10 mm and faces posteromedially. The second depression lies anteroventrally in respect to the former, and faces medially. Its outline is circular and measures c. 7 mm by 7 mm. Both depressions possess a distinct rim. The ventral aspect of the callus also shows several small round to oval-shaped depressions. If these depressions underlie a pathologic origin, the current morphology is consistent with lesions caused by osteomyelitis (Ortner & Putschar, 1981; Pschyrembel, 1990; Rothschild & Martin, 2006).

In the left pedal phalanx IV-1, there are two bulbous swellings on the lateral side (Fig. 9F). One is positioned underneath and posteroventral to the lateral ligament pit, another one is situated at the posterolateral side near the proximal articulation. The anterior swelling follows the slightly sinuous curvature of the ventral side of the bone in lateral view, which is the result of the constricted phalangeal shaft between the proximal and distal joints, which are both dorsoventrally expanded in relation to the shaft. The posterior swelling parallels the posterolateral and lateral margin of the proximal articulation, and is therefore vertically oriented. The swellings are separated by a small oblique gap, under which the bone seems to have retained its usual form. Both swellings have a smooth surface structure not different from other parts of the bone, but are not found on the same element of the right foot and are therefore abnormal. The swellings are different from the callus on the left pedal phalanx II-2, as they have a clearly delimited and abrupt border to either side. As additionally no lesions are found and a fracture line is absent, the pathology on the left pedal phalanx IV-1 is classified as idiopathic.

Discussion

Identification and cause of pathologies

According to the scheme of Hanna (2002), the pathologic elements of SMA 0005 can be classified as follows: the fifth cervical vertebra, the scapula, several ribs and right ischium are traumatic, and the callus structure of the left pedal phalanx II-2 is traumatic-infectious. In contrast, the supposed pathologies in the lower jaw and in the reduced flexor tubercle of the left pedal phalanx II-2 cannot be assigned to a certain type of this scheme, as they show evidence of advanced healing. They are most likely traumatic or developmental in origin. The same is true for the abnormal outgrowths in the neural arch of the fourth cervical, which are most likely developmental in origin or idiopathic. The pathology on the left humerus is infectious or idiopathic, whereas the left pedal phalanx IV-1 is classified as idiopathic. With exception of the ischium, all traumatic / traumatic-infectious pathologic elements show unambiguous evidences of healing, indicating that the respective pathologies did not cause the death of SMA 0005. The role of the ischial fracture as a possible cause of death will be discussed below.

The deformed anterior end of the left dentary of SMA 0005 is most likely pathologic, but no obvious lesions are developed. This indicates that the supposed pathology was probably completely healed and happened long before the animal died. A pathology in the anterior part of the dentary is also found in the *Allosaurus* specimen USNM 2315 (Gilmore, 1920; Tanke & Currie, 2000; Molnar, 2001). As in SMA 0005, the symphysial region is strongly deformed, leading to a concavity in the anterior part of the dentary, which is bordered anteriorly by a dorsally pointing, hook-like projection. The anterior alveoli are completely resorbed so that the symphysial region is edentulous. According to Gilmore (1920) and Tanke & Currie (2000) the anterior end of the dentary in USNM 2315 was probably bitten off and then heavily remodelled during the healing process. As no sign of other pathologic deformations are visible in the anterior end of the dentary, the supposed trauma happened probably long before the death of the animal, too. Assuming a similar scenario for the supposed pathology in SMA 0005, both specimens may indicate face-biting behaviour in *Allosaurus*, which was previously also hypothesized for other large-bodied theropods (e.g. *Sinraptor*, *Albertosaurus*, *Daspletosaurus*, *Gorgosaurus* and *Tyrannosaurus*), including in juveniles of some of these taxa (Tanke & Currie, 2000; Peterson et al., 2009; Bell, 2010). Another example of a remodeled alveolus with possible traumatic origin was recently described for a single maxilla of the basal tetanuran *Sinosaurus* (= "*Dilophosaurus sinensis*") (Xing et al., 2013). However, it is also possible that the abnormal shape of the dentary in SMA 0005 results from developmental malformation or a fracture that happened in earlier ontogeny, which left no remaining traces.

The deformation of the anterior end of the dentary has implications for the structure and function of the mandibular symphysis in *Allosaurus*. As pointed out by Holliday & Nesbitt (2013), most basal theropod dinosaurs have a very simple mandibular symphysis that consists of a simple flattened medial area of the anterior end of the dentary. However, even in such an osteologically simple structure the actual union of the left and right mandible by connective tissue can be quite variable (see Holliday et al., 2010). The deformation of the left, but not the right mandible in SMA 0005 indicates that there was no very tight junction between the two mandibular rami, and the symphysis and the jaws as a whole functioned despite the different morphologies and resulting differences in the level of the alveolar margins in the left and right mandible. This is also supported by the deformation seen in USNM 2315, which also affected the mandibular symphysis.

Another interesting aspect of the pathologic dentary of SMA 0005 is its similarity with dentaries of spinosaurid megalosaurs. As there are no direct indications of pathology in the bone itself, and the pathologic nature can only be inferred by comparison with the other dentary, which shows a more typical morphology for *Allosaurus*. This element, if found isolated, would probably not have been classified as *Allosaurus*. This has happened with the dentary USNM 2315, which was originally described as a new species, *Labrosaurus ferox*, by Marsh (1884). Thus, caution is needed when evaluating the systematic position of isolated elements to rule out possible pathologies.

The most common pathology in the axial skeleton of dinosaurs is the fusion of single vertebrae, which often appears in the caudal series. Possible causes of vertebral fusion are e.g. congenital abnormality (e.g. Witzmann et al., 2008), infections (Rothschild, 1997; Rothschild & Martin, 2006), malformations during the healing process of a trauma (Rothschild, 1997; Butler et al., 2013), diffuse idiopathic skeletal hyperostosis (DISH) (Rothschild, 1987; Rothschild & Berman, 1991) or spondyloarthropathy (Rothschild & Martin, 2006; Witzmann et al., 2014). No evidence of vertebral fusion is found in SMA 0005.

Like in the *Allosaurus* specimen MOR 693, the dorsal neural spines of SMA 0005 show irregular-shaped exostoses, which were diagnosed by Hanna (2002) as idiopathic pathological ossification of interspinous ligaments. However, little research has been done on the classification of ossified ligaments and other soft tissues in dinosaurs. In ornithopods and dromeosaurid theropod dinosaurs, ossified tendons are found to stiffen parts of the axial skeleton, and these structures are commonly not interpreted as pathologic (e.g. Ostrom, 1969; Norell & Makovicky, 1999; Organ, 2006). However, in many theropod dinosaurs, rugose outgrowths are found on the anterior and posterior sides of the neural spine, which are thought to be part of ossified prespinal and postspinal ligaments, respectively. These structures occur more frequently on larger specimens (e.g. *Allosaurus* BYU 725/12901, BYU 725/12902, BYU 725/13051, UMNH VP 8365, UMNH VP 13813; *Acrocanthosaurus* SMU 74646, Harris 1998; cf. *Spinosaurus* BSPG 2006 I 57), although there are also smaller specimens with such ossification (e.g.

Allosaurus UMNH VP 7341, DINO 11541). In individuals preserving an articulated or associated vertebral series, no clear pattern of intervertebral tendon ossifications can be observed. In *Neovenator*, the posterior cervical vertebrae show ossifications at the apexes of the neural spines, and most dorsal vertebrae show such structures (Brusatte, Benson & Hutt, 2008), while in *Baryonyx*, a mid-cervical vertebra (BMNH R9951) shows relatively large ossifications, whereas more posterior positioned vertebrae lack such structures and only show rugose attachment sites for the respective ligaments on the neural arch (Charig & Milner, 1997). In some cases, the interspinal ossifications have been suggested to be of diagnostic and thus taxonomic value (Chure, 2000). The above cases show that ligament ossifications in dinosaurs are frequently not interpreted as pathologic, and because many theropods show ossifications of at least the attachment areas of interspinal ligaments, we advocate that they should be regarded as non-pathologic, pending more detailed research on the topic.

However, the exostoses found in the fourth cervical of SMA 0005 differ in their position and morphology from the examples mentioned above. Here, the strongly irregular shape of the anterior exostosis resembles the morphology of an osteochondroma, which represents the most common type of bone tumours in humans (Murphey et al., 2000; Sekharappa et al., 2014). In captive wild extant mammals and reptiles (including birds), however, the development of tumours is rather rare (Ratcliffe, 1933; Effron, Griner & Benirschke, 1977; Huchzermeyer, 2003). Thus, it is not surprising that the unambiguous diagnosis of tumours in dinosaurs is limited to only a few cases (e.g. Rothschild et al., 1998; Rothschild, Witzke & Hershkovitz, 1999; Rothschild et al., 2003; Arbour & Currie, 2011; Rega, 2012). Due to the restricted knowledge of tumour formation in dinosaurs in general, this diagnosis has to be seen with caution. However, if the diagnosis is correct, the anterior exostosis found in the fourth cervical of SMA 0005 represents the third case of an osteochondroma in dinosaurs (Rega, 2012). The smaller, more regular-shaped exostosis on the posterior side of the neural arch does not fulfil the criteria for a bone tumour. One possible explanation for these structures could be an inflammatory ossification of the *ligamentum elasticum interlaminare*, which attaches right above the neural canal of cervical vertebrae (Tsuihiji, 2004), probably affecting the neck mobility. However, if none of the presented diagnosis is correct, both exostoses have to be classified as idiopathic.

Evidence for traumatic pathologies in the vertebral column is also rare in dinosaurs. Carpenter et al. (2005) describes an anterior caudal of *Allosaurus* with a possible puncture in the left transversal process, which was most likely injured by a *Stegosaurus* tail spike, indicating a predator-prey relationship between both dinosaurs. Traumatic caudals found in the basal sauropodomorph *Massospondylus* (Butler et al., 2013) and the hadrosaur *Edmontosaurus* (Carpenter, 2000) probably result from unsuccessful attacks of large-bodied theropods, indicating active hunting behaviour in the latter, while an injured caudal in the abelisaurid *Majungasaurus* (Farke & O'Connor, 2007) may indicate cannibalistic behaviour. In contrast, the traumatic fracture found in the fifth cervical of SMA 0005 probably results from a serious accident. Although the whole left postzygapophysis was basically broken, the trauma shows evidence of healing in form of a callus, indicating the survival of the accident. A possible explanation for such a rather unusual break might be found in the importance of the neck in hunting behaviour in large theropods (e.g. Snively & Russell, 2007a,b; Snively et al., 2013). Thus, the injury might have resulted from a failed hunting attack or from struggling prey, in which case this represents further evidence for active hunting in *Allosaurus* (see also Carpenter et al., 2005). However this may be, the severity of the injury most probably had a serious affect on the neck mobility of the specimen (see Snively et al., 2013).

Fractured or infected presacral ribs are one of the most common pathologies found within theropods (Molnar, 2001), in which, however, cervical ribs are less affected than dorsal elements. Pathologic cervical ribs are reported for *Megalosaurus* (Tanke & Rothschild, 2002), *Allosaurus* (Petersen et al., 1972) and *Tyrannosaurus* (Brochu, 2003), whereas corresponding dorsal rib pathologies are found in various large-bodied theropods like the abelisaurid *Majungasaurus* (Farke & O'Connor, 2007), the allosauroids *Acrocanthosaurus* (Harris, 1998), *Allosaurus* (Molnar, 2001; Hanna, 2002; Rothschild & Tanke, 2005), *Mapusaurus* (Bell & Coria, 2013) and *Sinraptor* (Currie & Zhao, 1993) and the tyrannosaurids *Albertosaurus* (Bell, 2010), *Gorgosaurus* (Lambe, 1917) and *Tyrannosaurus* (Brochu, 2003; Rothschild & Molnar, 2008). The examples mentioned above show different kinds of pathologies, i.e. trauma-related callus formations (Harris, 1998; Hanna, 2002; Brochu, 2003), pseudarthroses (Harris, 1998; Brochu, 2003; Rothschild & Molnar, 2008; Bell, 2010) or lesions by microbial infections (Harris, 1998; Hanna, 2002; Brochu, 2003; Bell & Coria, 2013), in which the latter could be the result of secondary infections of the injury. Hanna (2002) further describes the formation of idiopathic spiculae on two fractured dorsal ribs in the *Allosaurus* specimen MOR 693. In SMA 0005, all pathologic ribs show evidence for traumatic-related pseudarthroses. Here, the pseudarthrosis as a healing response (rather than callus healing) in the cervical rib results most likely from regular neck movements (Snively & Russell, 2007a; Snively et al., 2013), whereas the pseudarthroses found in the dorsal ribs were probably caused by constant movement of the ribcage during breathing (Claessens, 2009a,b) or due to thorax movements during locomotion (see Mallison, 2010).

The fractured scapula shows a clear case of a pseudarthrosis as healing response, which resulted from the apparent malunion of the fractured elements. Mechanical loading is additionally likely, as the proximal fragment, which is articulated with the rest of the arm, is tilted ventrally. The extent of the malunion may be indicative of syn-traumatic displacement, which potentially indicates great destructive force acting upon the element. Accordingly, the left arm in SMA 0005 was likely dysfunctional after the trauma. Other examples of pathologic scapulae in theropods can be found in the *Allosaurus* specimen USNM 4734 (Gilmore, 1920; Rothschild, 1997; Molnar, 2001) and in *Yangchuanosaurus* (Xing et al., 2009). The scapula of USNM 4734 shows a strong, arched dislocation between both fragments, in which the proximal element developed a spine-like exostosis on the ventral margin of the projecting portion of the proximal fragment (Gilmore, 1920; Rothschild, 1997). In contrast, the injury of the scapula in *Yangchuanosaurus* shows callus formation as healing response (Xing et al., 2009), indicating an incipient fracture. Other examples of pathologic scapulae seem not to be related to traumatic events, but with the development of exostoses [e.g. *Acrocanthosaurus* (NCSM 14345, pers. obs.) and *Neovantor* (Brusatte et al., 2008)], idiopathic lesions [e.g. *Allosaurus* (MOR 693; Hanna, 2002)] and infectious lesions in relation to osteomyelitis [e.g. *Allosaurus* (UUVP 1528, UUVP 5599, Molnar, 2001; Hanna, 2002)].

Because the injuries of the left scapula and the dorsal ribs from the left side are present at almost the same level of the thorax, it is possible that these traumas happened in one single event, e.g. a serious fall, or a defensive blow from a sauropod tail. This scenario would be even more probable if the deformations found in the other dorsal ribs from the left side have a traumatic origin. However, as stated above, this cannot currently be confirmed, as they cannot be distinguished from taphonomic deformations. Multiple rib fractures from one thorax side are also documented in *Acrocanthosaurus* (Harris, 1998), *Allosaurus* (Hanna, 2002) and *Tyrannosaurus* (Brochu, 2003), possibly resulting from one single traumatic event.

The most complex pathology appears in the left pedal phalanx II-2, including a reduced flexor tubercle, a callus formation of the phalangeal shaft, and several lesions penetrating the callus. The origin of the reduced flexor tubercle remains speculative, possibly being developmental in origin or resulting from a healed trauma. However, as the flexor tubercle in its normal condition should prevent the hyperextension of pedal phalanges, it is possible that the reduced process in SMA 0005 was not able to fulfil this task properly, leading to a frequent overloading of pedal muscles and ligaments. Thus, it is possible that this pathology is physically linked to the callus formation in the proximal portion of the phalangeal shaft. This type of pathology is very common in theropods (Madsen, 1976; Rothschild, 1988; Rothschild et al., 2001; Rothschild & Tanke, 2005; Farke & O'Connor, 2007; Bell, 2010; Zanno et al., 2011; Anné et al., 2014), and probably a result of stress fractures related to strenuous activities (Rothschild et al., 2001; Rothschild & Tanke, 2005). The additional penetration of the callus by several lesions indicate a secondary infection of the pedal phalanx, perhaps caused by a syn-traumatic injury of adjacent soft tissue, through which microbial pathogens got access to the bone and cause contiguous osteomyelitis. Thus, the callus pathology is most likely traumatic-infectious. Secondary infections of callus structures in, as well as infections not clearly linkable to fractures, seem to be common in pedal phalanges of *Allosaurus* (MOR 693, UUVP 1657, UMNH VP 6295, UMNH VP 6284, UMNH VP 10755, UMNH VP 6287, UMNH

VP 6299). In two specimens (MOR 693; UUVP 1657), the secondary infections led to colossal exostoses, causing chronic pain and restriction in the locomotion.

The cause for the abnormalities of the left humerus and left pedal phalanx IV-1 are unknown, although the pits found on the ulnar condyle of the left humerus might result from an infection.

The most severe and potentially fatal pathology occurs in the ischium, which most likely represents a traumatic fracture. Pathologies in the pelvic region are not often documented in theropods and usually restricted to the ilium (Molnar, 2001; Hanna, 2002; Bell & Coria, 2013). In the *Allosaurus* specimen UUVP 5985, the ilium is fused with the ischium (Hanna, 2002). However, an ischial fracture is to our knowledge not documented within theropods so far. The fracture of the right ischium exhibits a large interfragmentary gap with a projecting fragment on the lateral side. Because unambiguous healing responses are absent around the fracture, the possibility that the ischium was broken post-mortem has to be considered. However, scenarios in which a skeletal element with a designated long axis fractures in the oblique way described above are hard to come by, and we think the most parsimonious explanation for the observed fracture is a traumatic event during life. This is perhaps supported by the presence of sandy sediment matrix in the interfragmentary gap, as a void would be expected to be filled by different material if the fracture was the result of stress related to tectonic activity. Although no callus structure is found around the fracture, its absence per se cannot be seen as a clear indicator for the lack of a healing response, as the integration of the ischium in a complex network of locomotor musculature (Carrano & Hutchinson, 2002; Hutchinson et al., 2005) would predict intense motion along the fracture, favoring the formation of a pseudarthrosis (Cleas et al., 2000; Loboa et al., 2001). As seen in the scapula, large parts of the fracture line can remain unfused in a pseudarthrosis, and the fragments can be adhered at the end points of overlapping fracture fragments. In SMA 0005, the periphery of the connective bone in the scapula is structurally marked by fine striations and modifications from the smooth surface of healthy bone. Unfortunately, the irregular texture of the ischium, which we interpret as taphonomic (see below), prevents an assessment of the bone structure around the area where the ischium fragments meet, as the pattern would have overprinted the original bone surface structure. Therefore, it cannot be clarified if the connection of the fragments is the result of incomplete fracturing, or a secondary bridging due to a healing response. As experimental studies on animal fractures have shown that overhanging fracture ends tend to be resorbed during the healing process (Loboa et al., 2001), the presence of a laterally projecting fragment indicates that the healing process, if already started, was still in an early phase, supporting the hypothesis that the trauma happened shortly before the animal died, and is accordingly a possible cause of death. It is likely that the locomotion ability of SMA 0005 was significantly limited or even inhibited by the injury, consequentially affecting life traits like its hunting success. The reason for the traumatic event remains speculative, although it must have been a forceful incident.

The irregular cortical texture found around the ischial fracture is probably not pathologic. The right pubis shows also large traces of similar structure. Smaller traces can be found in the right coracoid, both scapulae, the left humerus, the left ischium, the left pubis and the left fibula (Fig. 5C, D). The structures differ in their morphology from the supposed lesions found the in right pedal phalanx II-2, as they possess a very irregular outline with a weak margin and a complex inner topography, which is composed of interconnected round pits with irregular size and depth (c. 1 to 3 mm). This morphology is similar to the superficial pits found on various sauropod bones from the Morrison Formation, which are most likely taphonomic in origin (Fiorillo, 1998; Hasiotis, Fiorillo & Hanna, 1999). Possible causes for these traces are bone corrosion due to soil acidity (Fiorillo, 1998) or scavenging by insect larvae (Hasiotis et al., 1999).

Implications for paleobiology and lifestyle

The number of pathologic specimens in general and the number of pathologies within fairly complete *Allosaurus* individuals suggest that members of this taxon had an active lifestyle predisposed to injury. Most pathologies found seem to be traumatic in origin, but only few show evidence of secondary infection (Molnar, 2001). This either suggests that inflamed wounds quickly caused death, leaving no osteological traces, or that the immune defence of these animals was successful in prohibiting infections. Oftentimes injuries were indeed survived, as evidence for healing responses are abundant in the theropod fossil record. In previous studies (e.g. Hanna, 2002; Butler et al., 2013; Vittore & Henderson, 2013) mammalian immune response has often been used as a model for explaining pathologic structures thought to be related to tissue-invasive microbial infections in non-avian dinosaur taxa. However, while the mammalian immune response to such infections usually is the formation of suppurative abscesses, extant reptiles (including birds) form small cysts of fibrin (fibriscesses) at the sources of infection, which tend to calcify in advance stages (Montali, 1988; Gomis et al., 1997; Huchzermeyer & Cooper, 2000; Cooper, 2005; Rega, 2012). Applying the extant phylogenetic bracket, a reptile-like immune response should be suspected for tissue-invasive microbial infections in non-avian dinosaurs, too. Consequently, application of a mammalian model for infectious pathologies in non-avian dinosaurs should be avoided (see Arbour & Currie, 2011; Rega, 2012). As the localization of pathogens in fibriscesses successfully prevents haematogenous osteomyelitis in reptiles, the risk of lethal infections due to the spread to other body regions is minimized (Rega, 2012). This is supported by the fact that theropods show only very localized indications for infections (Molnar, 2001).

The severity of pathologies in SMA 0005 and other *Allosaurus* specimens (Gilmore, 1920; Molnar, 2001; Hanna, 2002) points to a frequent exposure to hazardous situations. This might be seen as evidence for an active predatory life style. If this is accepted, many of the traumatic pathologies found could be the result of hunting accidents (see e.g. Carpenter et al., 2005). Some of the pathologies seen in *Allosaurus*, like the broken cervical postzygapophysis and scapula of SMA 0005, the hypertrophied pedal phalanx of MOR 693 (Hanna, 2002) and UMNH 1657 (Madsen, 1976; Hanna, 2002), or the fibula of USNM 4734 (Gilmore, 1920) can be expected to severely limit the movement, manoeuvrability, and speed of the animals. This in turn should affect the hunting success, but also intra- and interspecific competition for various other resources (water, territories, captured prey and carrion) of such an individual, which would be expected to mean certain death within a relatively short period of time. This is especially true for animals with solitary behavior. Indeed, the broken ischium qualifies as a strongly limiting and severe injury, and is potentially related to the death of SMA 0005. However, the number of cases of advanced healing for severe injuries within various *Allosaurus* specimens (including SMA 0005) might be an indication of social behaviour, in which prey was shared among individuals of a group. Although stratigraphic and taphonomic information is not provided in detail for all *Allosaurus* remains, this taxon represents the most abundant theropod within the Morrison Formation, and oftentimes appears with several specimens within near proximity to one another (see Gilmore, 1920; Madsen, 1976; Foster, 2003; Loewen, 2009), supporting a possible gregarious behavior. Within theropod dinosaurs, similar behavior has been further hypothesized for the coelophysoids *Coelophysis* (Colbert, 1989) and *Syntarsus* (Raath, 1990), the carcharodontosaurid *Mapusaurus* (Coria & Currie, 2006), the ornithomimosaur *Sinornithomimus* (Kobayashi & Lü, 2003; Varricchio et al., 2008), and the tyrannosaurids *Albertosaurus* (Currie, 2000; Currie & Eberth, 2010) and *Daspletosaurus* (Currie et al., 2005), which were all found in (nearly) monospecific assemblages. Although monospecific assemblages are scarce in the Morrison Formation (Foster, 2003; Gates, 2005), at least the Cleveland-Lloyd Dinosaur Quarry is by far dominated by *Allosaurus*. In spite of repeated taphonomic and sedimentological investigations of the quarry (Bilbey, 1998, 1999; Gates, 2005), the abundance of *Allosaurus* has not been satisfactorily explained, so that a gregarious scenario should not be ruled out at this point.

Conclusions

The *Allosaurus* SMA 0005 represents a further specimen of this taxon with multiple pathologies, which were mostly traumatic in origin and pertain to all body regions (i.e. skull, axial skeleton, pectoral and pelvic girdle, and extremities). Traces of healing responses in all pathologic bones but the ischium suggest the survival of accidents and infections, but also an active predatory lifestyle predisposed to injury. The scarcity and local restriction of infectious pathologies is in agreement with a reptile-like immune response preventing the spread of infections via the blood stream. The survival of injuries affecting the physical fitness in *Allosaurus* may indicate gregarious behavior. However, verification of this hypothesis would require more direct evidence, like an unambiguous find of a group or direct trackway evidence (e.g. McCrea et al., 2014). The probable fracture in the ischium was potentially fatal, as no advanced traces of healing could be identified.

Acknowledgements

We would like to thank Hans 'Kirby' Siber, Thomas Bolliger (both Sauriermuseum Aathal) and entire Aathal team for access to SMA 0005 and logistic support. We further thank Philipp Schütz (EMPA) for assisting during the CT scans, Randy Irmis and Carrie Levitt-Bussian (both Utah Museum of Natural History), Brooks Britt and Rodney Scheetz (both Brigham Young University), and Jack Horner and John Scanella (Museum of the Rockys) for access other *Allosaurus* material as well as Vince Schneider and Lindsay Zanno (both North Carolina Museum of Natural Sciences) for sharing pictures of *Acrocanthosaurus*, and Roger Benson (University of Oxford) for sharing pictures of *Neovenator*. Finally, we want to acknowledge Mark Loewen (Utah Museum of Natural History), Richard Butler (University of Birmingham) and Judith Engmann (Medizinische Hochschule Hannover) and for discussions. This study was supported by the Volkswagen Foundation under grant I/84 640 (to O.W.M.R.).

References

Anné J, Edwards NP, Wogelius RA, Tumarkin-Deratzian AR, Sellers WI, van Veelen A, Bergmann U, Sokaras D, Alonso-Mori R, Ignatyev K et al. 2014. Synchrotron imaging reveals bone healing and remodelling strategies in extinct and extant vertebrates. *Journal of the Royal Society Interface* 11:1-10.

Arbour VM, Currie PJ. 2011. Tail and pelvis pathologies of ankylosaurian dinosaurs. *Historical Biology* 23:375-390.

Avilla LS, Fernandes R, Ramos DFB. 2004. Bite marks on a crocodylomorph from the Upper Cretaceous of Brazil: evidence of social behavior? *Journal of Vertebrate Paleontology* 24:971-973.

Bell PR. 2010. Palaeopathological changes in a population of *Albertosaurus sarcophagus* from the Upper Cretaceous Horseshoe Canyon Formation of Alberta, Canada. *Canadian Journal of Earth Sciences* 47:1263-1268.

Bell PR, Coria RA. 2013. Palaeopathological survey of a population of *Mapusaurus* (Theropoda: Carcharodontosauridae) from the Late Cretaceous Huincul Formation, Argentina. *PLoS ONE* 8:e63409.

Bilbey SA. 1998. Cleveland-Lloyd Dinosaur Quarry - age, stratigraphy and depositional enviroments. *Modern Geology* 22:87-120.

Bilbey SA. 1999. Taphonomy of the Cleveland-Lloyd Dinosaur Quarry in the Morrison Formation, central Utah - a lethal spring-fed pond. In: Gillette DD ed. *Vertebrate Paleontology in Utah*. Salt Lake City: Miscellaneous Publication, 121-133.

Breithaupt BH. 1997. Howe Quarry. In: Currie PJ, Padian K eds. *Encyclopedia of Dinosaurs*. San Diego: Academic Press, 355-356.

Brochu CA. 2003. Osteology of *Tyrannosaurus rex*: insights from a nearly complete ckeleton and high-resolution computed tomographie analysis of the skull. *Society of Vertebrate Paleontology Memoir* 7:1-138.

Brown B. 1935. Sinclair dinosaur expedition, 1934. *Natural History* 36:2-15.

Brusatte SL, Benson RBJ, Hutt S. 2008. The osteology of *Neovenator salerii* (Dinosauria: Theropoda) from the Wealden Group (Barremian) of the Isle of Wight. *Monograph of the Palaeontological Society* 162:1-75.

Burch SH. 2014. Complete forelimb myology of the basal theropod dinosaur *Tawa hallae* based on a novel robust muscle reconstruction method. *Journal of Anatomy* 225:271-297.

Butler RJ, Yates AM, Rauhut OWM, Foth C. 2013. A pathological tail in a basal sauropodomorph dinosaur from South Africa: evidence of traumatic amputation? *Journal of Vertebrate Paleontology* 33:224-228.

Carpenter K. 2000. Evidence of predatory behavior by carnivorous dinosaurs. *Gaia* 15:135-144.

Carpenter K, Sanders F, McWhinney LA, Wood L. 2005. Evidence for predator-prey relationships. Examples for *Allosaurus* and *Stegosaurus*. In: Carpenter K ed. *The carnivorous dinosaurs*. Bloomington: Indiana University Press, 325-350.

Carrano MT, Hutchinson JR. 2002. Pelvic and hindlimb musculature of *Tyrannosaurus rex* (Dinosauria: Theropoda). *Journal of Morphology* 253:207-228.

Charig AJ, Milner AC. 1997. *Baryonyx walkeri*, a fish-eating dinosaur from the Wealden of Surrey. *Bulletin of the Natural History Museum Geology* 53:11-70.

Chure DJ. 2000. A new species of *Allosaurus* from the Morrison Formation of Dinosaur National Monument (UT-CO) and a revision of the theropod family Allosauridae. Columbia University.

Claessens LPAM. 2009a. A cineradiographic study of lung ventilation in *Alligator mississippiensis*. *Journal of Experimental Zoology* 311A:563-585.

Claessens LPAM. 2009b. The skeletal kinematics of lung ventilation in three basal bird taxa (emu, tinamou, and guinea fowl). *Journal of Experimental Zoology* 311A:586-599.

Cleas L, Wolf S, Augat P. 2000. Mechanische Einflüsse auf die Callusheilung. *Chirurg* 71:989-994.

Colbert EH. 1989. The Triassic dinosaur *Coelophysis*. *Museum of Northern Arizona Bulletin* 57:1-160.

Cooper RG. 2005. Bacterial, fungal and parasitic infections in the ostrich (Struthio camelus var. domesticus). *Animal Science Journal* 76:97-106.

Coria RA, Currie PJ. 2006. A new carcharodontosaurid (Dinosauria, Theropoda) from the Upper Cretaceous of Argentina. *Geodiversitas* 28:71-118.

Currie PJ. 2000. Possible evidence of gregarious behavior in tyrannosaurids. *Gaia* 15:271-277.

Currie PJ, Eberth DA. 2010. On gregarious behavior in *Albertosaurus*. *Canadian Journal of Earth Sciences* 47:1277-1289.

Currie PJ, Zhao X. 1993. A new carnosaur (Dinosauria, Theropoda) from the Jurassic of Xinjiang, People's Republic of China. *Canadian Journal of Earth Sciences* 30:2037-2081.

Currie PJ, Trexler D, Koppelhus EB, Wicks K, Murphy N. 2005. An unusual multi-individual tyrannosaurid bonebed in the Two Medicine Formation (Late Cretaceous, Campanian) of Montana (USA). In: Carpenter K ed. *The carnivorous dinosaurs*. Bloomington: Indiana University Press, 313-324.

Effron M, Griner L, Benirschke K. 1977. Nature and rate of neoplasia found in captive wild mammals, birds, and reptiles at necropsy. *Journal of the National Cancer Institute* 59:185-198.

Evers S, Foth C, Rauhut OWM, Pabst B, Mateus O. 2013. Traumatic pathologies in the postcranium of an adult *Allosaurus* specimen from the Morrison Formation of the Howe Quarry, Wyoming, U.S.A. *Journal of Vertebrate Paleontology, Program and Abstracts* 33:124.

Farke AA. 2004. Horn use in *Triceratops* (Dinosauria: Ceratopsidae): testing behavioral hypotheses using scale models. *Palaeontologia Electronica* 7:1-10.

Farke AA, O'Connor PM. 2007. Pathology in *Majungasaurus crenatissimus* (Theropoda: Albelisauridae) from the Late Cretaceous of Madagascar. *Journal of Vertebrate Paleontology* 27:180-184.

Fiorillo AR. 1998. Bone modification features on sauropod remains (Dinosauria) from the Freezeout Hills Quarry N (Morrison Formation) of southeastern Wyoming and their contribution to fine-scale paleoenvironmental interpretation. *Modern Geology* 23:111-126.

Foster JR. 2003. Paleoecological analysis of the vertebrate fauna of the Morrison Formation (Upper Jurassic), Rocky Mountain Region, U.S.A. *New Mexico Museum of Natural History and Science, Bulletin* 23:1-95.

Gates TA. 2005. The Late Jurassic Cleveland-Lloyd Dinosaur Quarry as a drought-induced assemblage. *Palaios* 20:363-375.

Gilmore GW. 1920. Osteology of the carnivorous dinosauria in the United States National Museum, with special reference to the genera *Antrodemus* (*Allosaurus*) and Ceratosaurus. *Bulletin of the United States National Museum* 110:1-159.

Gomis SM, Goodhpe R, Kumor L, Caddy N, Riddell C, Potter AA, Allan BJ. 1997. Isolation of *Escherichia coli* from cellulitis and other lesions of the same bird in broilers at slaughter. *The Canadian Veterinary Journal* 38:159-162.

Gross JD, Rich TH, Vickers-Rich P. 1993. Dinosaur bone infection. *National Geographic Research & Exploration* 9:286-293.

Hanna RR. 2002. Multiple injury and infection in a sub adult theropod dinosaur *Allosaurus fragilis* with comparisons to allosaur pathology in the Cleveland-Lloyd Dinosaur Quarry Collection. *Journal of Vertebrate Paleontology* 22:76-90.

Harris JD. 1998. A reanalysis of *Acrocanthosaurus atokensis*, its phylogenetic status, and paleobiological implications, based on a new specimen from Texas. *New Mexico Museum of Natural History and Science, Bulletin* 13:1–75.

Hasiotis ST, Fiorillo AR, Hanna RR. 1999. Preliminary report on borings in Jurassic dinosaur bones: evidence for invertebrate-vertebrate interactions. In: Gillette DD ed. *Vertebrate Paleontology in Utah*. Salt Lake City: Miscellaneous Publication, 193-200.

Holliday CM, Nesbitt SJ. 2013. Morphology and diversity of the mandibular symphysis of archosauriforms. *Geological Society, London, Special Publications* 379:1-18.

Holliday CM, Gardner NM, Paesani SM, Douthitt M, Ratliff JL. 2010. Microanatomy of the mandibular symphysis in lizards: patterns in fiber orientation and Meckel's cartilage and their significance in cranial evolution. *The Anatomical Record* 293:1350-1359.

Huchzermeyer FW. 2003. *Crocodiles*. Wallingford: CABI Publishing.

Huchzermeyer FW, Cooper JA. 2000. Fibricess, not abcess, resulting from a localised inflammatory response to infection in reptiles and birds. *Veterinary Record* 147:515-517.

Hutchinson JR, Anderson FC, Blemker SS, Delp SL. 2005. Analysis of hindlimb muscle moment arms in *Tyrannosaurus rex* using a three-demensional musculoskeletal computer model: implications for stance, gait, and speed. *Paleobiology* 31:676-701.

Klein P, Schell H, Streitparth F, Heller M, Kassi J-P, Kandziora F, Bragulla H, Haas NP, Duda GN. 2003. The initial phase of fracture healing is specifically sensitive to mechanical conditions. *Journal of Orthopaedic Research* 21:662-669.

Kobayashi Y, Lü J. 2003. A new ornithomimid dinosaur with gregarious habits from the Late Cretaceous of China. *Acta Palaeontologica Polonica* 48:235–259.

Lambe LM. 1917. The Cretaceous theropodous dinosaur *Gorgosaurus*. *Geological Survey of Canada, Memoir* 100:1-84.

Loboa EG, Beaupré GS, Carter DR. 2001. Mechanobiology of initial pseudoarthrosis formation with oblique fracture. *Journal of Orthopaedic Research* 19:1067-1072.

Loewen MA. 2009. Variation in the Late Jurassic theropod dinosaur *Allosaurus*: ontogenetic, functional, and taxonomic implications. University of Utah.

Madsen JHJ. 1976. *Allosaurus fragilis*: a revised osteology. *Utah Geological and Mineralogical Survey Bulletin* 109:3-163.

Mallison H. 2010. The digital *Plateosaurus* II: An assessment of the range of motion of the limbs and vertebral column and of previous reconstructions using a digital skeletal mount. *Acta Palaeontologica Polonica* 55:433-458.

Marsh OC. 1884. Principal characters of American Jurassic dinosaurs. Part 8. The order Theropoda. *American Journal of Science* 27:329-341.

McCrea RT, Buckley LG, Farlow JO, Lockley MG, Currie PJ, Matthews NA, Pemberton SG. 2014. A “terror of tyrannosaurs”: the first trackways of tyrannosaurids and evidence of gregariousness and pathology in Tyrannosauridae. *PLoS ONE* 9:e103613.

McKibbin B. 1978. The biology of fracture healing in long bones. *The Journal of Bone and Joint Surgery* 60:150-162.

Molnar RE. 2001. Theropod paleopathology: a literature survey. In: Tanke DH, Carpenter K eds. *Mesozoic Vertebrate Life*. Bloomington: Indiana University Press, 337-363.

Molnar RE, Farlow JO. 1990. Carnosaur paleobiology. In: Weishampel DB, Dodson P, Osmólska H eds. *The Dinosauria*. Berkeley: University of California Press, 210-224.

Montali RJ. 1988. Comparative pathology of inflammation in the higher vertebrates (reptiles, birds and mammals). *Journal of Comparative Pathology* 99:1-26.

Moodie RL. 1923. *Paleopathology: an introduction to the study of ancient evidences of disease*. Urbana: University of Illinois Press.

Murphey MD, Choi JJ, Kransdorf MJ, Flemming DJ, Gannon FH. 2000. Imaging of osteochondroma: variants and complications with radiologic-pathologic correlation. *Radiographics* 20:1407-1434.

Norell MA, Makovicky PJ. 1999. Important features of the dromaeosaurid skeleton II: information from newly collected specimens of *Velociraptor mongoliensis*. *American Museum Novitates* 3282:1-45.

Organ CL. 2006. Thoracic epaxial muscles in living archosaurs and ornithopod dinosaurs. *The Anatomical Record, Part A* 288A:782-793.

Ortner DJ, Putschar WGJ. 1981. *Identification of pathological conditions in human skeletal remains*. Washington, D. C.: Smithsonian Institution Press.

Ostrom JH. 1969. Osteology of *Deinonychus antirrhopus*, an unusual theropod from the Lower Cretaceous of Montana. *Peabody Museum of Natural History, Bulletin* 30:1-165.

Park S-H, O'Connor K, McKellop H, Sarmiento A. 1998. The Influence of active shear or compressive motion on fracture-healing. *The Journal of Bone and Joint Surgery* 80:868-878.

Petersen K, Isakson JI, Madsen JHJ. 1972. Perliminary study of paleopathologies in the Cleveland-Lloyd dinosaur collection. *Utah Academy Proceedings* 49:44-47.

Peterson JE, Henderson MD, Scherer EP, Vittore CP. 2009. Face biting on a juvenile tyrannosaurid and behavioral implications. *Palaios* 24:780-784.

Pschyrembel W. 1990. *Klinisches Wörterbuch*. Berlin: Walter de Gruyter & Co.

Raath MA. 1990. Morphological variation in small theropods and its meaning in systemtics: evidence from *Syntarsus rhodesiensis*. In: Carpenter K, Currie PJ eds. *Dinosaur systematics: approaches and perspectives*. Cambridge: Cambridge University Press, 91-105.

Ratcliffe HL. 1933. Incidence and nature of tumors in captive wild mammals and birds. *The American Journal of Cancer* 17:116-135.

Rega E. 2012. Disease in dinosaurs. In: Brett-Surman MK, Holtz TRJ, Farlow JO eds. *The complete dinosaur*. Bloomington: Indiana University Press, 666-711.

Remes K. 2008. Evolution of the pectoral girdle and forelimb in Sauropodomorpha (Dinosauria, Saurischia): osteology, myology and function. Ludwig-Maximilians-Universität, München.

Rothschild BM. 1987. Diffuse idiopathic skeletal hyperostosis as reflected in the paleontologic record: dinosaurs and early mammals. *Seminars in Arthritis and Rheumatism* 17:119-125.

Rothschild BM. 1988. Stress fracture in a ceratopsian phalanx. *Journal of Paleontology* 62:302-303.

Rothschild BM. 1997. Dinosaurian paleopathology. In: Farlow JO, Brett-Surman MK eds. *The complete dinosaur*. Bloomington: Indiana University Press, 426-448.

Rothschild BM, Berman DS. 1991. Fusion of caudal vertebrae in Late Jurassic sauropods. *Journal of Vertebrate Paleontology* 11:29-36.

Rothschild BM, Martin LD. 1993. *Paleopathology: disease in the fossil record*. Ann Arbor: CRC Press.

Rothschild BM, Martin LD. 2006. Skeletal impact of disease. *New Mexico Museum of Natural History and Science, Bulletin* 33:1-226.

Rothschild BM, Molnar RE. 2008. Tyrannosaurid pathologies as clues to nature and nurture in the Cretaceous. In: Larson P, Carpenter K eds. *Tyrannosaurus rex, the tyrant king*. Bloomington: Indiana University Press, 286-304.

Rothschild BM, Storrs GW. 2003. Decompression syndrome in plesiosaurs (Sauropterygia: Reptilia). *Journal of Vertebrate Paleontology* 23:324-328.

Rothschild BM, Tanke DH. 2005. Theropod paleopathology. In: Carpenter K ed. *The carnivorous dinosaurs*. Bloomington: Indiana University Press, 351-365.

Rothschild BM, Tanke DH, Ford TL. 2001. Theropod stress fractures and tendon avulsions as a clue to activity. In: Tanke DH, Carpenter K eds. *Mesozoic Vertebrate Life*. Bloomington: Indiana University Press, 331-336.

Rothschild BM, Tanke DH, Helbling M, Martin LD. 2003. Epidemiologic study of tumors in dinosaurs. *Naturwissenschaften* 90:495-500.

Rothschild BM, Tanke DH, Hershkovitz I, Schultz M. 1998. Mesozoic neoplasia: origins of haemangioma in the Jurassic age. *The Lancet* 351:1862.

Rothschild BM, Witzke BJ, Hershkovitz I. 1999. Metastatic cancer in the Jurassic. *The Lancet* 354:398.

Schell H, Epari DR, Kassi JP, Bragulla H, Bail HJ, Duda GN. 2005. The course of bone healing is influenced by the initial shear fixation stability. *Journal of Orthopaedic Research* 23:1022-1028.

Sekharappa V, Amritanand R, Krishnan V, David KS. 2014. Symptomatic solitary osteochondroma of the subaxial cervical spine in a 52-year-old patient. *Asian Spine Journal* 8:84-88.

Sereno PC, Beck AL, Dutheil DB, Gado B, Larsson HCE, Lyon GH, Marcot JD, Rauhut OWM, Sadleir RW, Sidor CA et al. 1998. A long-snouted predatory dinosaur from Africa and the evolution of Spinosaurids. *Science* 282:1298-1302.

Snively E, Russel AP. 2007a. Functional variation of neck muscles and their relation to feeding style in Tyrannosauridae and other large theropod dinosaurs. *The Anatomical Record* 290:934-957.

Snively E, Russell AP. 2007b. Craniocervical feeding dynamics of *Tyrannosaurus rex*. *Paleobiology* 33:610-638.

Snively E, Cotton JR, Ridgely RC, Witmer LM. 2013. Multibody dynamics model of head and neck function in *Allosaurus* (Dinosauria, Theropoda). *Palaeontologia Electronica* 16:1-29.

Stromer E. 1915. Ergebnisse der Forschungsreisen Prof. Stromers in den Wüsten Ägyptens. II Wirbeltier-Reste der Baharîje-Stufe (unterstes Cenoman). 3. Das Original des Theropoden *Spinosaurus aegyptiacus* nov. gen., nov. spec. *Abhandlungen der Königlich Bayerischen Akademie der Wissenschaften. Mathematisch-physikalische Klasse* 28:1-32.

Strube P, Sentuerk U, Riha T, Kaspar K, Mueller M, Kasper G, Matziolis G, Duda GN, Perka C. 2008. Influence of age and mechanical stability on bone defect healing: age reverses mechanical effects. *Bone* 42:758-764.

Tanke DH, Currie PJ. 2000. Head-biting behavior in theropod dinosaurs: paleopathological evidence. *Gaia* 15:167-184.

Tanke DH, Rothschild BM. 2002. DINOSORES: An annotated bibliography of dinosaur paleopathology and related topics, 1838-2001. *New Mexico Museum of Natural History and Science, Bulletin* 20:1-96.

Tsuihiji T. 2004. The ligament system in the neck of *Rhea americana* and its implication for the bifurcated neural spines of sauropod dinosaurs. *Journal of Vertebrate Paleontology* 24:165-172.

Varricchio DJ, Sereno PC, Zhao X, Tan L, Wilson JA, Lyon GH. 2008. Mud-trapped herd captures evidence of distinctive dinosaur sociality. *Acta Palaeontologica Polonica* 53:478-567.

Vittore CP, Henderson MD. 2013. Brodie abscess involving a tyrannosaur phalanx: imaging and implications. In: Parrish JM, Molnar RE, Currie PJ, Koppelhus EB eds. *Tyrannosaurid paleobiology*. Bloomington: Indiana University Press, 223-236.

Witzmann F, Asbach P, Remes K, Hampe O, Hilger A, Paulke A. 2008. Vertebral pathology in an ornithopod dinosaur: a hemivertebra in *Dysalotosaurus lettowvorbecki* from the Jurassic of Tanzania. *The Anatomical Record* 291:1149-1155.

Witzmann F, Claeson KM, Hampe O, Wieder F, Hilger A, Manke I, Niederhagen M, Rothschild BM, Asbach P. 2011. Paget disease of bone in a Jurassic dinosaur. *Current Biology* 21:R647-R648.

Witzmann F, Schwarz-Wings D, Hampe O, Fritsch G, Asbach P. 2014. Evidence of spondyloarthropathy in the spine of a phytosaur (Reptilia: Archosauriformes) from the Late Triassic of Halberstadt, Germany. *PLoS ONE* 9:e85511.

Wolff EDS, Salisbury SW, Horner JR, Varricchio DJ. 2009. Common avian infection plagued the tyrant dinosaurs. *PLoS ONE* 4:e7288.

Xing L, Bell PR, Rothschild BM, Ran H, Zhang J, Dong Z, Zhang W, Currie PJ. 2013. Tooth loss and alveolar remodeling in *Sinosaurus triassicus* (Dinosauria: Theropoda) from the Lower Jurassic strata of the Lufeng Basin, China. *Chinese Science Bulletin* 58:1931-1935.

Xing L, Dong H, Peng G, Shu C, Hu X, Jiang H. 2009. A scapular fracture in *Yangchuanosaurus hepingensis* (Dinosauria: Theropoda). *Geological Bulletin of China* 28:1390-1395.

Zanno LE, Varricchio DJ, O'Connor PM, Titus AL, Knell MJ. 2011. A New troodontid theropod, *Talos sampsoni* gen. et sp. nov., from the Upper Cretaceous Western Interior Basin of North America. *PLoS ONE* 6:e24487.

Figures

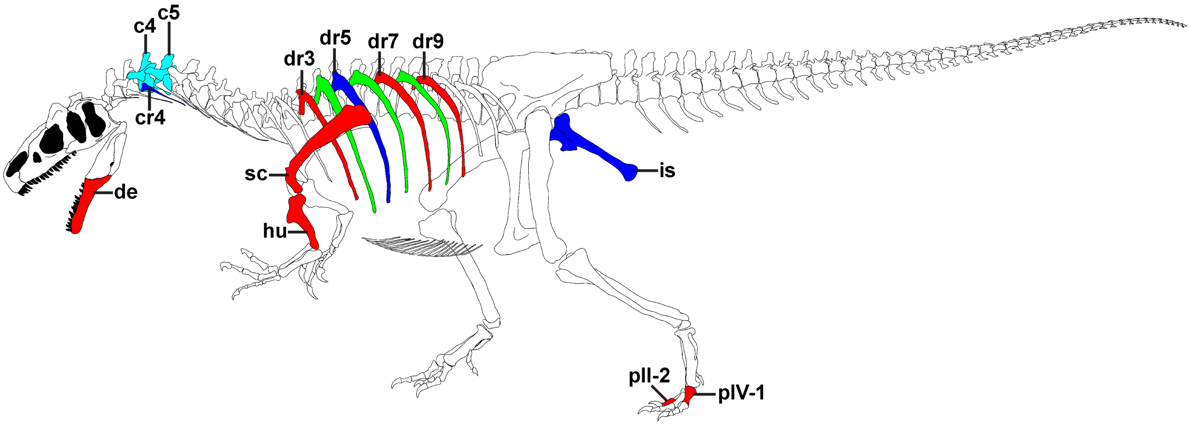

Figure 1 Overview of pathologies in SMA 0005. Skeletal reconstruction of SMA 0005, showing all pathologic bones. Pathologic elements from the left side are shown in red, while respective elements from the right side are marked in blue. Unpaired pathologic bones are colored in cyan. Green ribs represent ribs from the left, for which a pathologic condition is uncertain. **Abbreviations: c** cervical, **cr** cervical rib, **de** dentary, **dr** dorsal rib, **hu** humerus, **is** ischium, **p** pedal phalanx, **sc** scapula. Skeletal reconstruction of SMA 0005 with courtesy from the Sauriermuseum Aathal.

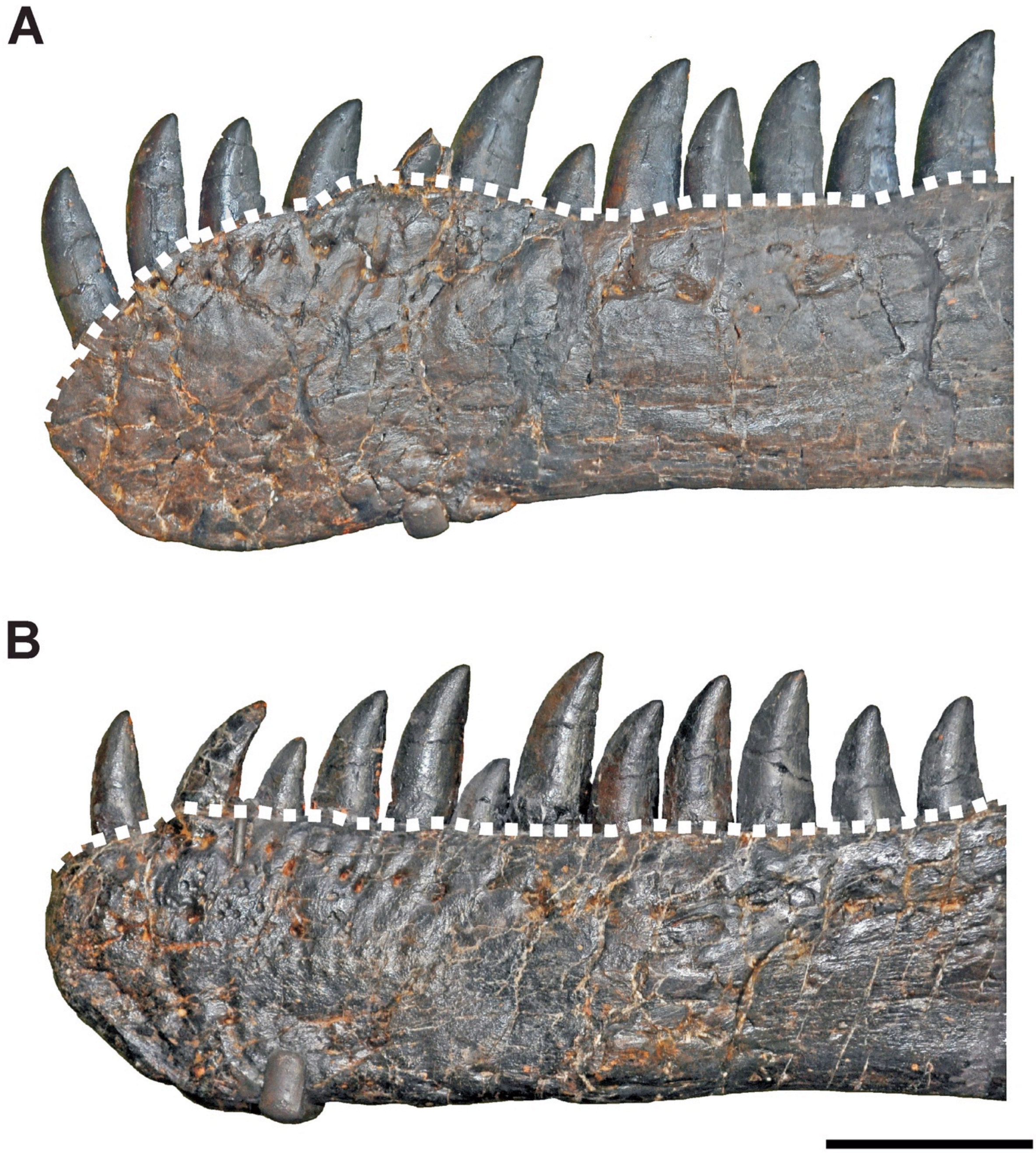

Figure 2 The dentaries of SMA 0005 in lateral view. (A) Left dentary with pathologic anterior end. (B) Right dentary in mirrored view, showing the normal condition for *Allosaurus*. The differences in the shape of the alveolar margin in both dentaries are shown with a dashed line. Note that most teeth in both dentaries are not original, but glued to the internal margin of the dentaries. Scale bar = 5 cm.

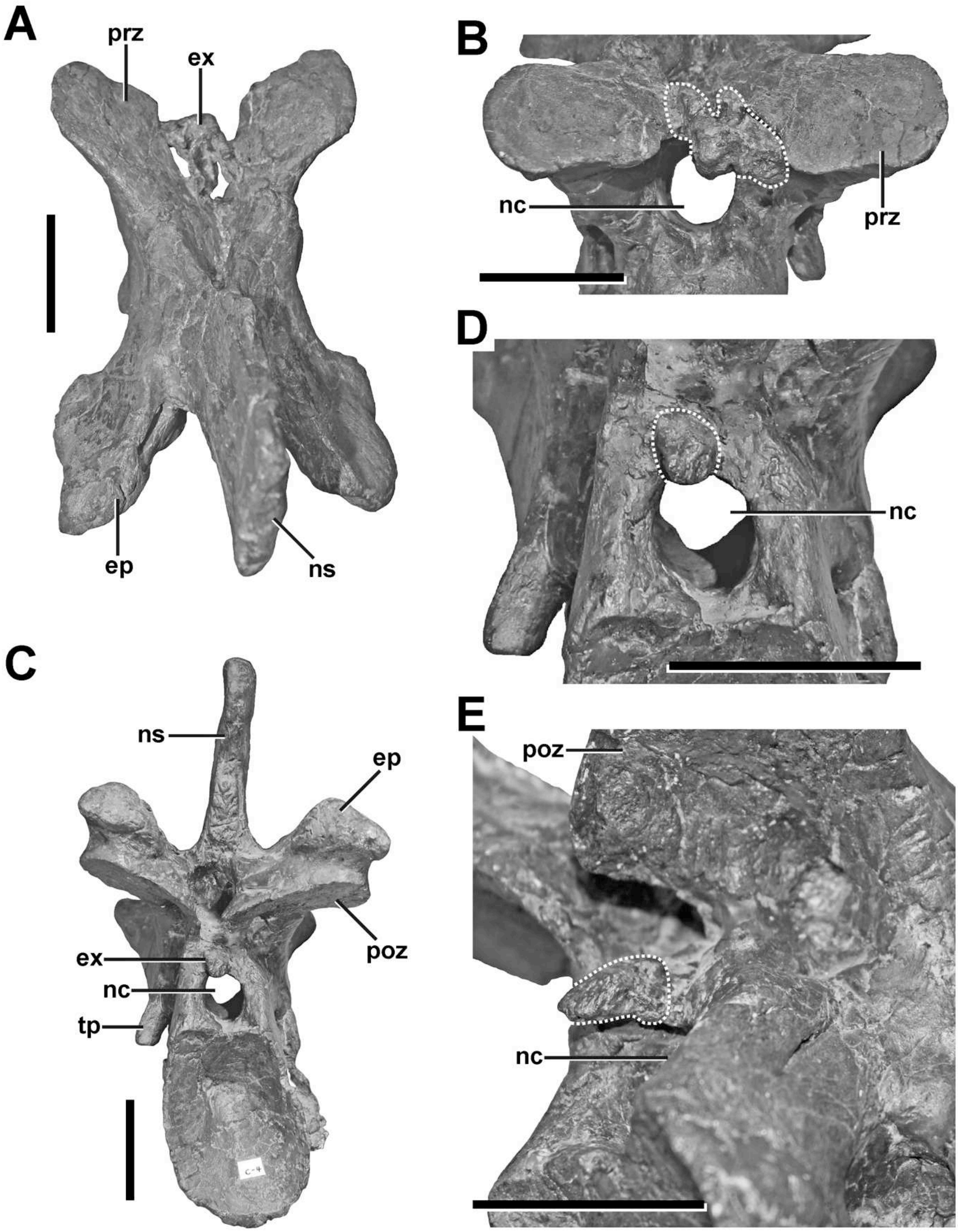

Figure 3 Fourth cervical of SMA 0005. (A) Fourth cervical in dorsal view, showing a pathologic exostosis (possible osteochondroma) between the prezygapophyses. (B) Possible osteochondroma from anterior view marked by a dotted line. (C) Fourth cervical in posterior view, showing another exostosis (possible inflammatory

ossification) above the neural canel. (D) Possible inflammatory ossification (dotted line) in close-view. (E) Possible inflammatory ossification (dotted line) in posterolateral view. **Abbreviations: ep** epipophysis, **ex** exostosis, **nc** neural canal, **ns** neural spine, **poz** postzygapophysis, **prz** prezygapophysis, **tp** transverse process. Scale bar = 5 cm.

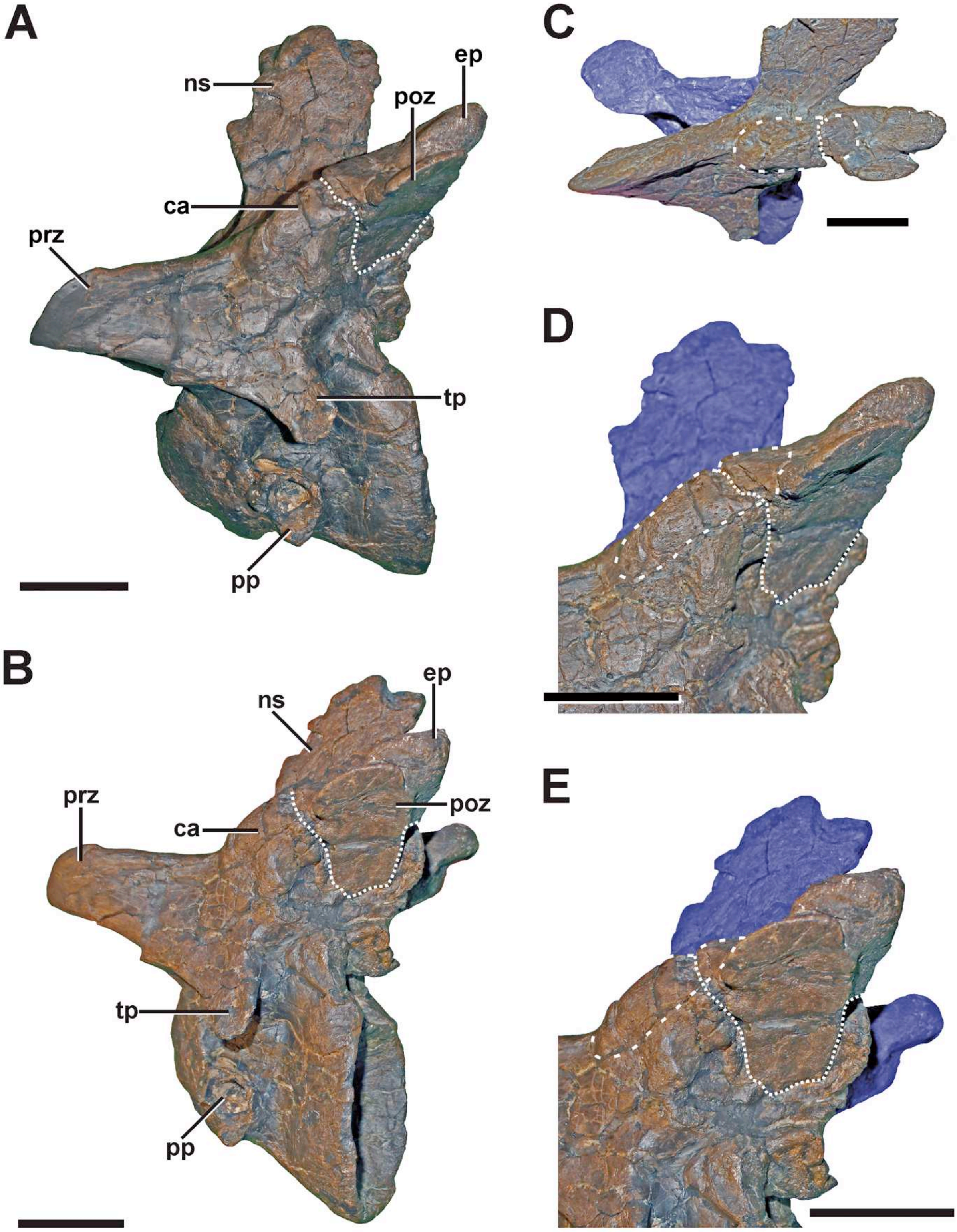

1026

1027 **Figure 4 Fifth cervical of SMA 0005.** (A) Fifth cervical in left lateral view, showing the

1028 callus and the fracture (dotted line) at the base of the left postzygapophysis. (B) Fifth

1029 cervical in lateral view in posterolateral view. (C) Callus (dashed line) and fracture

1030 (dotted line) in laterodorsal view. (D) Callus (dashed line) and fracture (dotted line) in lateroventral view. (E) Callus (dashed line) and fracture (dotted line) in oblique posterolateral view. Parts of the bone are colored for better contrast. **Abbreviations: ca** callus, **ep** epipophysis, **ns** neural spine, **poz** postzygapophysis, **pp** parapophysis, **prz** prezygapophysis, **tp** transverse process. Scale bar = 5 cm.

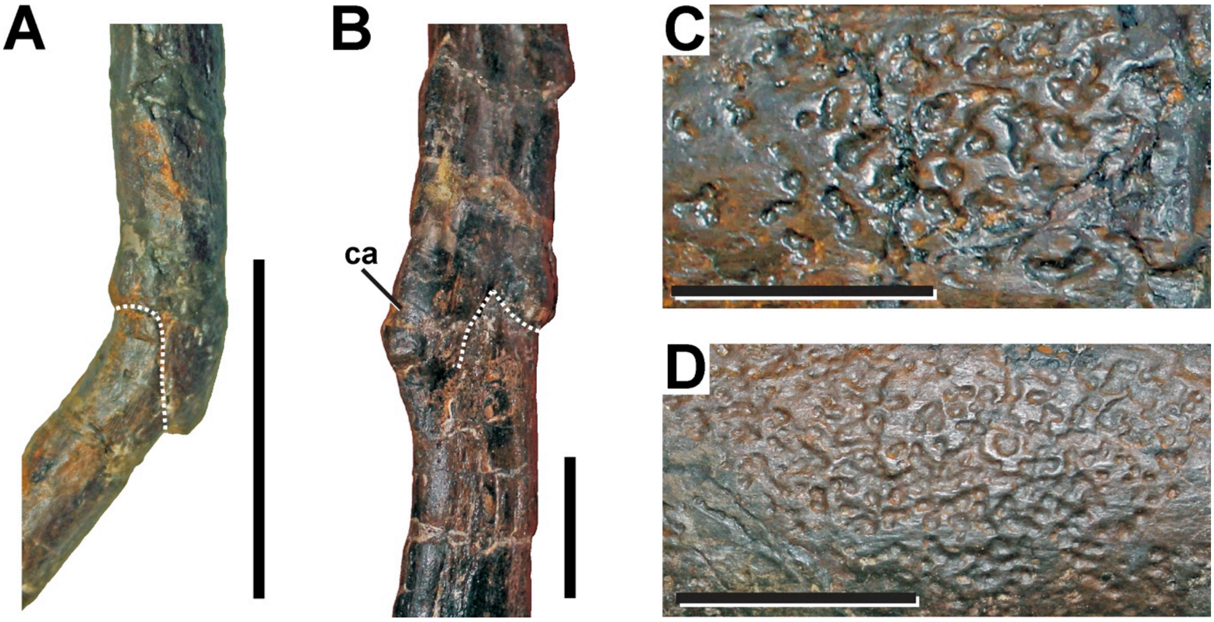

Figure 5 Pathologic ribs and cortical traces in SMA 0005. (A) Fourth cervical rib from the right side with fracture (dotted line). (B) Seventh dorsal rib from the left side with fracture (dotted line). (C) Cortical traces in the right ischium. (D) Cortical traces in the left scapula. **Abbreviations: ca** callus. Scale bar = 2 cm.

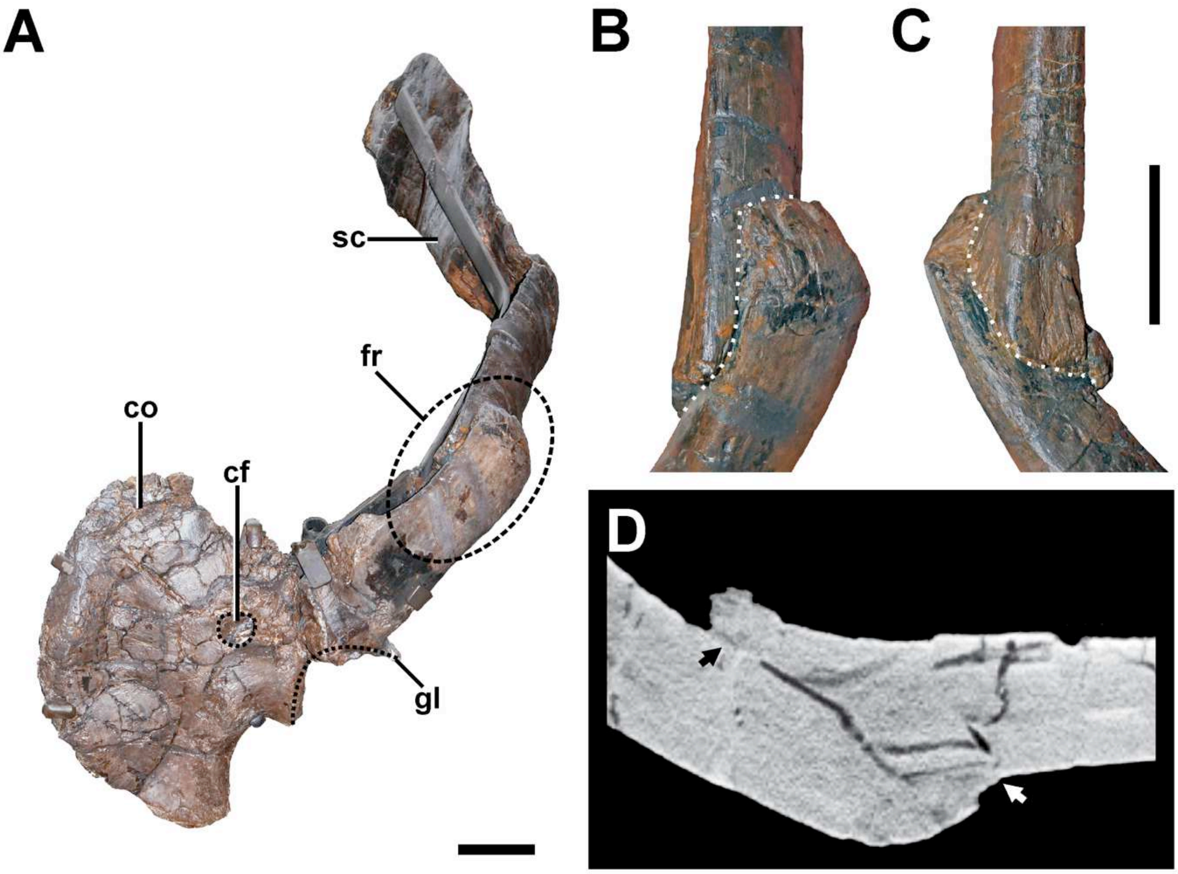

Figure 6 Pathologic scapula of SMA 0005. (A) Left scapula in anterolateral view, showing the fractured area of the scapula blade (dashed line). (B) Fracture (dotted line) in dorsal view. (C) Fracture (dotted line) in ventral view. (D) CT scan of the scapula, showing that only the fracture ends constitute a fused bridge between the fracture elements (arrows), which is consistent with a pseudarthrosis. **Abbreviations: co** coracoid, **cf** coracoid foramen, **fr** fracture, **gl** glenoid facet, **sc** scapula blade. Scale bar = 5 cm.

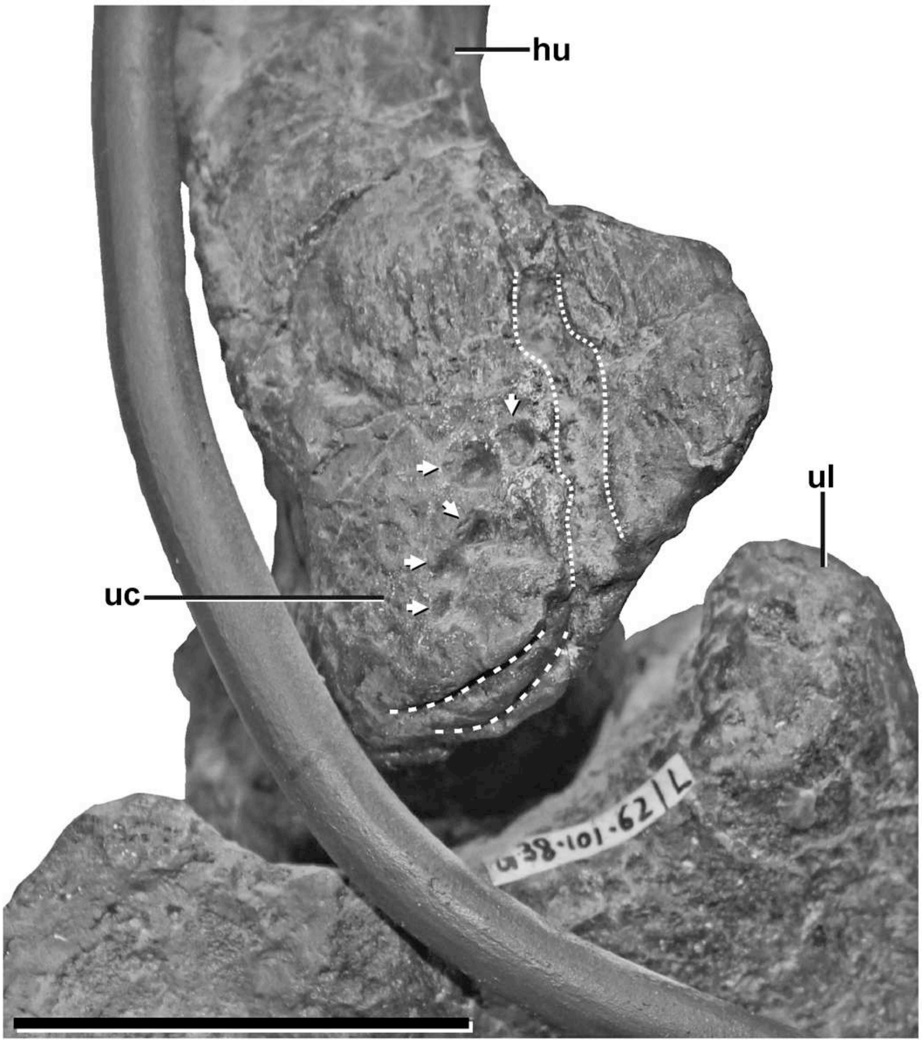

Figure 7 Pathologic structures in the left humerus of SMA 0005. Proximal portion of the humerus in ventromedial view, showing idiopathic pathologies. The pathologies contain an irregular cortical texture with numerous pits (arrows), a deep oblique groove toward the anterior aspect of the medial side (dotted lines), and two sharp, trough-like marks on the ventral surface of the ulnar condyle (dashed lines). **Abbreviations: hu** humerus, **ul** ulna, **uc** ulnar condyle. Scale bar = 5 cm.

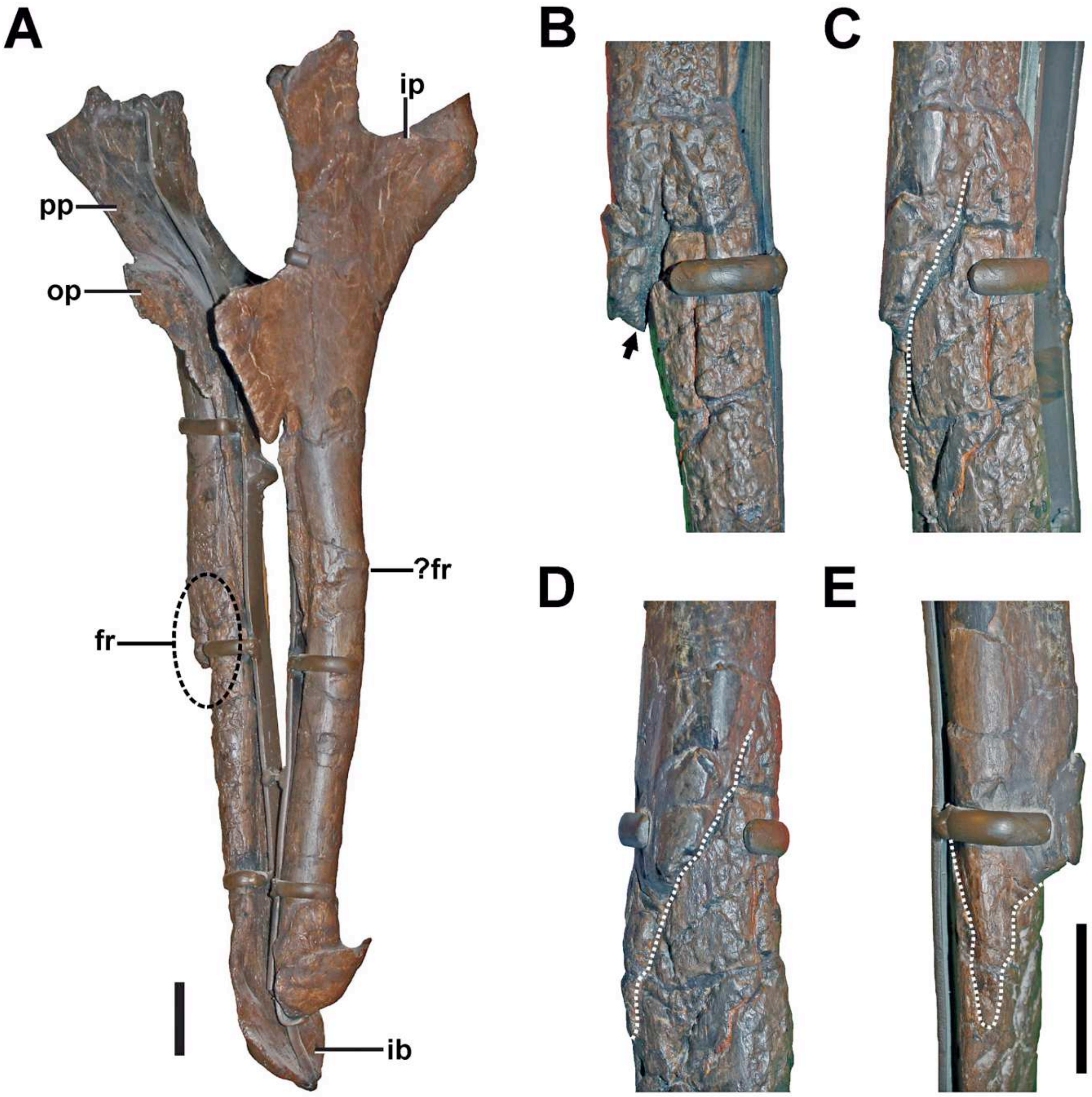

Figure 8 Ischium of SMA 0005. (A) Both Ischia in anterolateral view, showing the oblique fracture at the shaft of the right ischium. (B) Interfragmentary gap (arrow) of the right ischium in anterior view. (C) Fracture (dotted line) of the right ischium in anterolateral view. (D) Fracture (dotted line) of the right ischium in lateral view. (E) Fracture (dotted line) of the right ischium in posterior view. **Abbreviations: fr** fracture, **ib** ischial boot, **ip** ischial peduncle, **op** obturator process **pp** pubic peduncle. Scale bar = 5 cm.

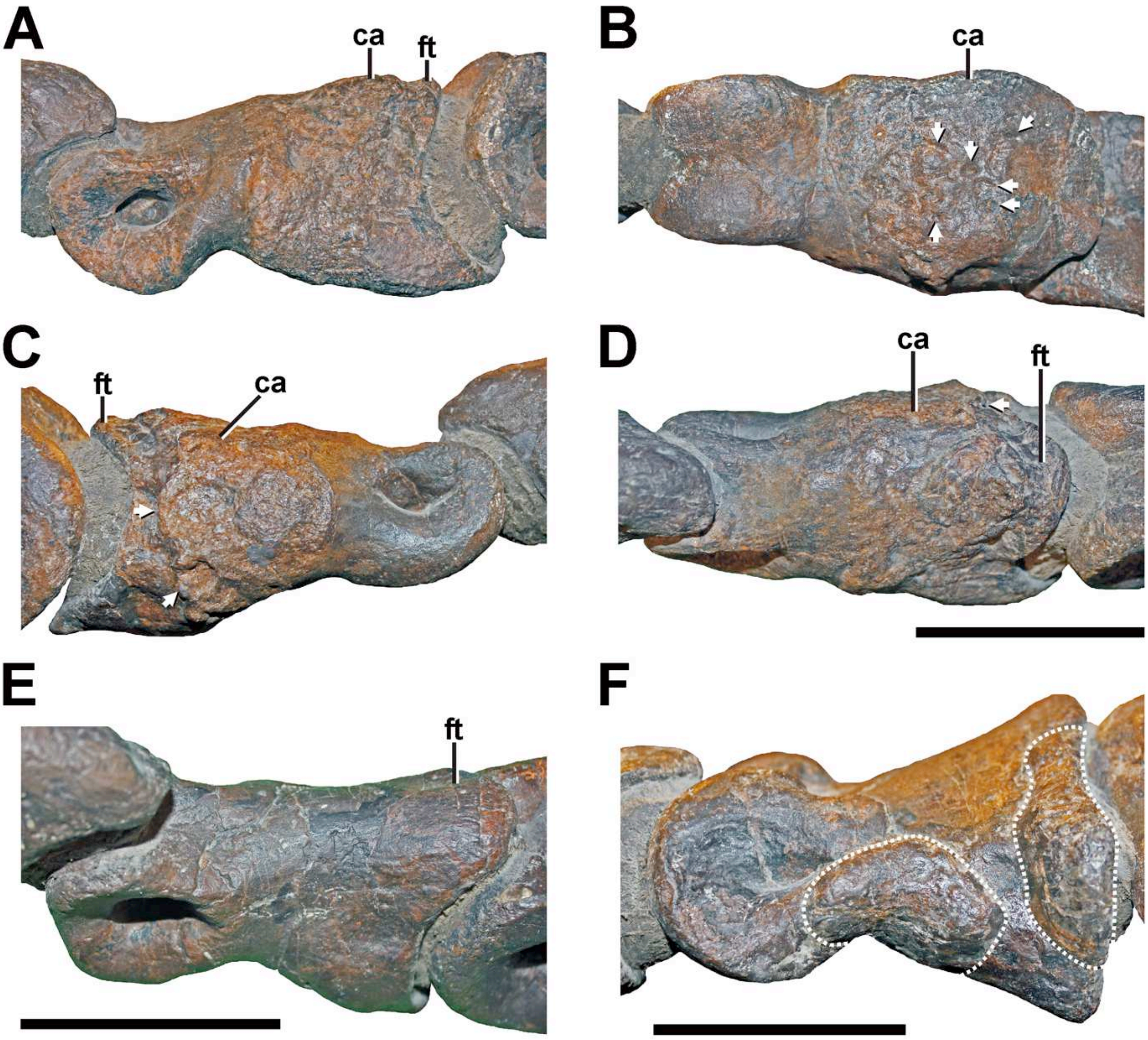

Figure 9 Pathologic phalanges in SMA 0005. (A) Left pedal phalanx II-2 from lateral view, showing the callus and the reduced flexor tubercle. (B) Left pedal phalanx II-2 from ventral view, showing the callus and multiple small pits (arrows). (C) Left pedal phalanx II-2 from medial view, showing the callus and two large depressions (arrows), possibly indicating a secondary infection of the bone. (D) Left pedal phalanx II-2 from dorsal view, showing the callus and one of the two large depressions on the medial side. (E) Right pedal phalanx II-2 from mediodorsal view, showing the normal condition and size of the flexor tubercle. (F) Left pedal phalanx IV-1 in lateral view, showing two idiopathic bulbous swellings (dotted lines). **Abbreviations: ca** callus, **ft** flexor tubercle. Scale bar = 5 cm.